

A General Framework for Temporal Fair User Scheduling in NOMA Systems

Shahram Shahsavari , Farhad Shirani , and Elza Erkip 

Abstract—Non-orthogonal multiple access (NOMA) is one of the promising radio access techniques for next generation wireless networks. Opportunistic multi-user scheduling is necessary to fully exploit multiplexing gains in NOMA systems, but compared with traditional scheduling, inter-relations between users' throughputs induced by multi-user interference poses new challenges in the design of NOMA schedulers. A successful NOMA scheduler has to carefully balance the following three objectives: Maximizing average system utility, satisfying desired fairness constraints among the users and enabling real time, and low computational cost implementations. In this paper, scheduling for NOMA systems under temporal fairness constraints is considered. Temporal fair scheduling leads to communication systems with predictable latency as opposed to utilitarian fair schedulers for which latency can be highly variable. It is shown that under temporal fairness constraints, optimal system utility is achieved using a class of opportunistic scheduling schemes called *threshold based strategies* (TBS). One of the challenges in heterogeneous NOMA scenarios—where only specific users may be activated simultaneously—is to determine the set of feasible temporal shares. A variable elimination algorithm is proposed to accomplish this task. Furthermore, an (online) iterative algorithm based on the Robbins–Monro method is proposed to construct a TBS by finding the optimal thresholds for a given system utility metric. The algorithm does not require knowledge of the users' channel statistics. Rather, at each time slot, it has access to the channel realizations in the previous time slots. Various numerical simulations of practical scenarios are provided to illustrate the effectiveness of the proposed NOMA scheduling in static and mobile scenarios.

Index Terms—Non-orthogonal multiple access, multi-user scheduling, temporal fairness, threshold-based strategies, Robbins–Monro algorithm.

I. INTRODUCTION

NON-orthogonal multiple access (NOMA) has emerged as one of the key enabling technologies for fifth generation wireless networks [1]–[4]. In order to satisfy the ever-growing demand for higher data rates in modern cellular systems, NOMA proposes serving multiple users in the same resource block. This is in contrast with conventional cellular systems which operate based on orthogonal multiple access (OMA) techniques such as

orthogonal frequency-division multiple access (OFDMA) [5]. In OMA systems, each time-frequency resource block is assigned to only one user in each cell, whereas, in NOMA systems, multiple users can be scheduled either in uplink (UL) or in downlink (DL) simultaneously [6]. As a result, the scheduler in the NOMA system may choose among a larger collection of users at each resource block as compared to an OMA one, often leading to a higher system throughput [7]. The high system throughput is due to NOMA multiplexing gains, achieved through a combination of superposition encoding strategies at the transmitter(s) and successive interference cancellation (SIC) decoding at the receiver(s) [7]–[9]. However, the inter-relations between users' throughputs induced by multi-user interference complicate the design of high-performance schedulers, giving rise to new challenges both in terms of designing user power allocation schemes [10]–[12] as well as optimal schedulers [2], [13]. Ideally, the scheduler is designed in tandem with the encoding and decoding strategies and power optimization techniques. However, due to the complexity of the problem, scheduling is usually studied in isolation assuming that the system throughputs are given to the scheduler based on a predetermined communication strategy [2], [14].

The objective of a NOMA scheduler is to maximize the system utility (e.g. system throughput) subject to the users' individual demand constraints, e.g. temporal demands or minimum utility demands. More precisely, at each resource block, the scheduler estimates the set of resulting system utilities from activating any specific subset of UL or DL users. It then chooses the set of active users in that block based on this information and users' individual fairness demands. Quantifying fairness in user scheduling has been a topic of significant interest. Various criteria on the users' quality of service (QoS) have been proposed to model and evaluate fairness of scheduling strategies. For OMA systems, scheduling under utilitarian [15], [16], proportional [17], [18], and temporal [19], [20] fairness criteria have been studied.

In delay sensitive applications, a system with reasonable and predictable latency may be more desirable than a system with highly variable latency, but potentially higher throughput. In such scenarios, temporally fair schedulers are often favored over utilitarian fair schedulers. Temporally fair schedulers provide each user with a minimum temporal share in order to control the average delay [21]. Furthermore, most of the power consumption in cellular devices is due to the radio electronics which are activated during data transmission and reception. Consequently, the maximum power drain of users can be restricted by considering upper-bounds on the users' temporal shares [20]. From

Manuscript received September 14, 2018; revised January 11, 2019 and February 22, 2019; accepted February 24, 2019. Date of publication March 7, 2019; date of current version May 22, 2019. This work was supported in part by the NYU WIRELESS Industrial Affiliates and in part by the National Science Foundation Grants EARS-1547332 and NeTS-1527750. The guest editor coordinating the review of this paper and approving it for publication was Dr. Zhiguo Ding. (Corresponding author: Farhad Shirani.)

The authors are with the Department of Electrical and Computer Engineering, New York University Tandon School of Engineering, New York, NY 10012 USA (e-mail: shahram.shahsavari@nyu.edu; fsc265@nyu.edu; elza@nyu.edu).

Digital Object Identifier 10.1109/JSTSP.2019.2903745

the perspective of the network provider, an additional upside of temporally fair schedulers is that users with low channel quality do not hinder network throughput as severely as in utilitarian fair schedulers [22]. There has been a significant body of work dedicated to the study of temporally fair schedulers in wireless local area networks [23], [24] and OMA cellular systems [20], [25], [26]. However, temporal fairness of NOMA schedulers, which is the topic of this paper, has not been investigated before.

In OMA systems, optimal utility subject to temporal demand constraints is achieved using a class of opportunistic scheduling strategies called *threshold based strategies* (TBS) [19]. An opportunistic scheduler exploits the time-varying nature of the users' wireless channels. In TBSs, at each resource block, the active user u_i is chosen based on the sum of two components: i) Performance value R_i (typically transmission rate), and ii) a constant term called the *user threshold* λ_i . The user thresholds are chosen to optimize the tradeoff between system utility and users' temporal share demands. The thresholds can be interpreted as the Lagrangian multipliers corresponding to the fairness constraints in the optimization of the system utility. In [19], a method based on the Robbins-Monro algorithm is proposed to construct optimal temporally fair TBSs for OMA systems.

In this work, we consider the user scheduling problem for NOMA systems under temporal fairness constraints. We provide a mathematical formulation of the problem which is applicable under general utility models and assumptions on the subsets of users which can be activated simultaneously. Our model is applicable to both UL and DL scenarios.

We first address the question of feasibility of a set of temporal demands in a given NOMA system. A vector of temporal shares is said to be *feasible* if there exists a scheduling strategy for which the resulting user temporal shares are equal to the elements of the vector. In OMA systems, since exactly one user is active at each block, a vector of temporal shares is feasible as long as its elements sum to less than or equal to one. However, in NOMA systems the set of feasible temporal shares is not trivially known. Determining the feasible set is especially challenging in large heterogeneous NOMA systems, where only specific users may be activated simultaneously. In Section IV-A, we propose a variable elimination method to derive the set of feasible temporal shares in arbitrary heterogeneous NOMA scenarios. Furthermore, we prove that given a feasible set of temporal demands, TBSs are optimal for NOMA systems. We further prove that any optimal scheduling strategy can be written in the form of a TBS.

The question of existence and construction of optimal NOMA TBSs is more challenging than OMA TBSs. The reason is that a NOMA TBS assigns a threshold to each subset of users which can be activated simultaneously, rather than each user separately. Therefore, in an optimal TBS the thresholds assigned to the subsets of users are inter-related. In Section V, we propose a construction method based on the Robbins-Monro algorithm to find the optimal thresholds for a NOMA TBS. The algorithm does not require knowledge of the users' channel statistics. Rather, at each time-slot, it has access to the channel realizations in the previous time-slots and updates the scheduler thresholds iteratively to construct the optimal TBS. In Section VI, we

consider practical NOMA systems where discrete modulation and coding strategies are used. In this case, the resulting system utilities are staircase functions of the users' signal to noise ratios. As a result, the utility from activating different subsets of users may lead to a tie in the TBS decision. This necessitates the design and optimization of a tie-breaking decision rule [19]. We propose a perturbation technique which circumvents the optimization and leads to TBSs whose average system utility is arbitrarily close to the optimal utility. In Section VII, we provide simulations and numerical examples in several practical scenarios involving static and mobile settings. We observe that the proposed scheduling algorithm adapts to the changes due to user mobility under typical velocity assumptions.

II. NOTATION

We represent random variables by capital letters such as X, U . Sets are denoted by calligraphic letters such as \mathcal{X}, \mathcal{U} . The set of natural numbers, and the real numbers are shown by \mathbb{N} , and \mathbb{R} respectively. The set of numbers $\{1, 2, \dots, n\}$, $n \in \mathbb{N}$ is represented by $[n]$. The closed interval $\{x : a \leq x \leq b\}$ is shown by $[a, b]$. The notation $[a, b]^n$ is used to denote the n -fold Cartesian product of the closed interval $[a, b]$ with itself. The vector (x_1, x_2, \dots, x_n) is written as x^n . The $m \times t$ matrix $[g_{i,j}]_{i \in [m], j \in [t]}$ is denoted by $g^{m \times t}$. For a random variable X , the corresponding probability space is $(\mathcal{X}, \mathbf{F}_X, P_X)$, where \mathbf{F}_X is the underlying σ -field. The set of all subsets of \mathcal{X} is written as $2^{\mathcal{X}}$. For an event $\mathcal{A} \in 2^{\mathcal{X}}$, the random variable $\mathbb{1}_{\mathcal{A}}$ is the indicator function of the event. We write $X \sim Unif[a, b]$ for a random variable X uniformly distributed on the interval $[a, b]$. Families of sets are shown using sans-serif letters (e.g. $\mathbf{X} = 2^{\mathcal{X}}$). Finally, $mod_k(i)$, $i, k \in \mathbb{N}$ represents the value of i modulo k .

III. SYSTEM MODEL

In this section, we describe the system model and formulate NOMA multi-user scheduling under temporal fairness constraints. We consider a single-cell time-slotted system with n users distributed within the cell. We define the user set as $\mathcal{U} = \{u_1, u_2, \dots, u_n\}$ where $u_i, i \in [n]$ denotes the i th user. At each time-slot, a subset of UL or DL users are activated simultaneously by the base station using NOMA. The maximum number of active users at each time-slot is bounded from above due to practical considerations such as latency and computational complexity at the scheduler and decoder. For example, the decoding complexity, communication delay under SIC, and the scheduler's computational complexity are proportional to the number of multiplexed users [1]. Consequently, only subsets of users with at most $N_{\max} \leq n$ elements can be activated simultaneously, where N_{\max} is determined based on the communication setup under consideration. Several works on NOMA scheduling consider $N_{\max} = 2$ and $N_{\max} = 3$ under various utilitarian and proportional fairness constraints [27], [28]. A subset of users which can be activated simultaneously is called a *virtual user*.

Definition 1 (Virtual User): For a NOMA system with n users and maximum number of active users $N_{\max} \leq n$, the set

of virtual users is defined as

$$\mathbf{V} = \{\mathcal{V}_j | j \in [m]\} = \{\mathcal{V}_j \subset \mathcal{U} | |\mathcal{V}_j| \leq N_{\max}\}.$$

The set $\mathcal{V}_j, j \in [m]$ is called the j th virtual user. The total number of virtual users in a NOMA system is equal to $m = \binom{n}{1} + \binom{n}{2} + \dots + \binom{n}{N_{\max}}$.

Our objective is to design a scheduler which maximizes the average network utility subject to temporal fairness constraints. At the beginning of each time-slot, the scheduler finds the utility due to activating each of the virtual users, and decides which virtual user to activate in that time-slot. The utility is usually defined as a function of the throughput of the elements of the virtual user.

Definition 2 (Performance Vector): The vector of jointly continuous variables $(R_{1,t}, R_{2,t}, \dots, R_{m,t}), t \in \mathbb{N}$ is the performance vector of the virtual users at time t . The sequence $(R_{1,t}, R_{2,t}, \dots, R_{m,t}), t \in \mathbb{N}$ is a sequence of independent¹ vectors distributed identically according to the joint density f_{R^m} .

Remark 1: It is assumed that the performance vector is bounded with probability one. Alternatively, we assume that $P(R^m \in [-M, M]^m) = 1$ for large enough $M \in \mathbb{R}_{\geq 0}$.

Remark 2: For the virtual user $\mathcal{V}_j = \{u_{i_1}, u_{i_2}, \dots, u_{i_{k_j}}\}$, $j \in [m], k_j \in [n], i_1, i_2, \dots, i_{k_j} \in [n]$, we sometimes write $\mathcal{V}_{i_1, i_2, \dots, i_{k_j}}(R_{i_1, i_2, \dots, i_{k_j}})$ instead of $\mathcal{V}_j(R_j)$ to represent the virtual user (performance variable).

The following example clarifies the notion of performance vector and provides a characterization for $(R_{1,t}, R_{2,t}, \dots, R_{m,t}), t \in \mathbb{N}$ in a large class of practical applications.

NOMA Downlink Scenario: In this example, we explicitly characterize the performance vector of a NOMA downlink system at any time-slot, where the system utility is defined to be the transmission sum-rate. The characterization can also be used for NOMA uplink scenarios with minor modifications (e.g. [29]). Let $h_{i,t}$ be the propagation channel coefficient between user u_i and the BS which captures small-scale and large-scale fading effects [30]. It is assumed that the channel coefficients $h_{i,t}, i \in [n]$ are independent over time. Let $R_{j,t}, j \in [m], t \in \mathbb{N}$ be the sum-rate of the elements of virtual user \mathcal{V}_j given that it is activated at time t . In NOMA downlink, a combination of superposition coding at the BS and SIC decoding at the mobile user has been proposed [31]. As envisioned for practical NOMA downlink systems, the decoding occurs in the order of increasing channel gains [7]. For a fixed virtual user $\mathcal{V}_j, j \in [m]$ and user $u_i \in \mathcal{V}_j$, let $\mathcal{I}_{j,t}^i$ be the set of elements of \mathcal{V}_j whose channels are stronger than that of u_i at time t . Alternatively, define $\mathcal{I}_{j,t}^i = \{u_l \in \mathcal{V}_j | |h_{l,t}| > |h_{i,t}|\}$. If \mathcal{V}_j is activated at time t , user u_i applies SIC to cancel the interference from users in \mathcal{V}_j whose channel gain is lower than that of u_i , hence only the signals from users in $\mathcal{I}_{j,t}^i$ are treated as noise and result in a lower transmission rate for u_i . It is well-known that in this scenario, the decoding strategy is optimal since the users' channels are degraded [32], [33]. The interested reader is referred to [9] for a

detailed description of optimal decoding strategies in the downlink scenario. The resulting signal to interference plus noise ratio (SINR) of user u_i is

$$\text{SINR}_{j,t}^i = \frac{P_{j,t}^i |h_{i,t}|^2}{|h_{i,t}|^2 \sum_{l \in \mathcal{I}_{j,t}^i} P_{j,t}^l + \sigma^2}, i \in \mathcal{V}_j, j \in [m], t \in \mathbb{N}, \quad (1)$$

where, $P_{j,t}^i$ denotes the transmit power assigned to u_i if virtual user \mathcal{V}_j is activated at time-slot t , and σ^2 is the noise power. Let $P_{j,t}^i$ denote the rate of user u_i if virtual user \mathcal{V}_j is activated at time-slot t , and let $R_{j,t}$ be the resulting sum-rate. Then,

$$R_{j,t}^i = \log_2(1 + \text{SINR}_{i,j,t}), i \in \mathcal{V}_j, j \in [m], \quad (2)$$

$$R_{j,t} = \sum_{i=1}^n R_{j,t}^i \mathbb{1}_{\{u_i \in \mathcal{V}_j\}}, j \in [m]. \quad (3)$$

Temporal fair scheduling guarantees that each user is activated for at least a predefined fraction of the time-slots. More precisely, user $u_i, i \in [n]$ is activated for at least \underline{w}_i of the time, where $\underline{w}_i \in [0, 1]$. Similarly, the scheduler guarantees that the users are not activated more than a predefined fraction of the time-slots which are given by the upper temporal share demands \bar{w}^n .

Definition 3 (Temporal Demand Vector): For an n user NOMA system, the vector \underline{w}^n (\bar{w}^n) is called the lower (upper) temporal demand vector.

The scheduler does not have access to the statistics of the performance vector f_{R^m} . Rather, at time-slot $t \in \mathbb{N}$, the scheduler takes $(R_{1,t}, R_{2,t}, \dots, R_{m,t}), k \in [t]$, the realizations of the performance vector in all time-slots up to time t and outputs the virtual user which is to be activated in the next time-slot. The NOMA scheduling setup is parametrized by $(n, N_{\max}, \underline{w}^n, \bar{w}^n, f_{R^m})$.

Definition 4 (Scheduling Strategy): A scheduling strategy (scheduler) $Q = (Q_t)_{t \in \mathbb{N}}$ for the scheduling setup parametrized by the tuple $(n, N_{\max}, \underline{w}^n, \bar{w}^n, f_{R^m})$ is a family of (possibly stochastic) functions $Q_t : \mathbb{R}^{m \times t} \rightarrow \mathbf{V}, t \in \mathbb{N}$, for which:

- The input to $Q_t, t \in \mathbb{N}$ is the matrix of performance vectors $R^{m \times t}$ which consists of t independently and identically distributed column vectors with distribution f_{R^m} .
- The temporal demand constraints are satisfied:

$$P(\underline{w}_i - \epsilon \leq \underline{A}_i^Q \leq \bar{w}_i + \epsilon, i \in [n]) = 1, \forall \epsilon > 0, \quad (4)$$

where, the temporal share of user $u_i, i \in [n]$ up to time $t \in \mathbb{N}$ is defined as

$$A_{i,t}^Q = \frac{1}{t} \sum_{k=1}^t \mathbb{1}_{\{u_i \in Q_k(R^{m \times k})\}}, \forall i \in [n], t \in \mathbb{N}, \quad (5)$$

and the average temporal share of user $u_i, i \in [n]$ is

$$\underline{A}_i^Q = \liminf_{t \rightarrow \infty} A_{i,t}^Q, \forall i \in [n]. \quad (6)$$

Note that analogous to Equation (6), one could define $\bar{A}_i^Q = \limsup_{t \rightarrow \infty} \bar{A}_{i,t}^Q, \forall i \in [n]$ and modify Equation (4) accordingly. However, as we will show in the next sections, for scheduling strategies of interest, we have $\underline{A}_i^Q = \bar{A}_i^Q$.

¹Note that the performance vector is assumed to be independent over time, meaning that at any two distinct time-slots, the performance vectors are independent of each other. However at a given time-slot the performance of the virtual users may be dependent with each other.

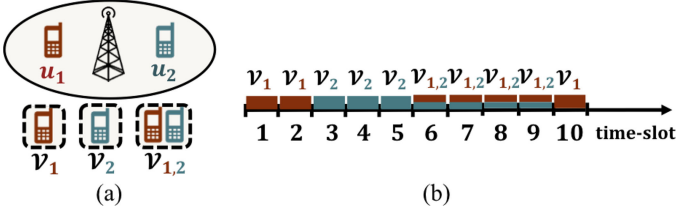


Fig. 1. (a) Two-user NOMA system with three virtual users. (b) Weighted Round Robin scheduling strategy when $\underline{w}_1 = \underline{w}_2 = 0.6$.

Remark 3: A scheduling setup where the temporal shares of users are required to take a specific value, i.e. $\underline{A}_i^Q = w_i, i \in [n]$, is called a scheduling setup with equality temporal constraints and is parametrized by $(n, N_{\max}, \underline{w}^n, \bar{w}^n, f_{R^m})$.

Definition 5 (System Utility): For a scheduling strategy Q :

- The average system utility up to time t , is defined as

$$U_t^Q = \frac{1}{t} \sum_{k=1}^t \sum_{j=1}^m R_{j,k} \mathbb{1}_{\{Q_k(R^{m \times k}) = v_j\}}. \quad (7)$$

- The average system utility is defined as

$$U^Q = \liminf_{t \rightarrow \infty} U_t^Q. \quad (8)$$

To further explain the notation, we provide an example of a weighted round robin scheduling strategy in a two-user NOMA scenario.

Example 1: Consider the downlink scenario shown in Figure 1. In this scenario $n = 2$, and $\mathcal{U} = \{u_1, u_2\}$. Furthermore, $m = 3$ and $\mathcal{V} = \{v_1, v_2, v_3\}$, where $v_1 = \{u_1\}$, $v_2 = \{u_2\}$, and $v_3 = v_{1,2} = \{u_1, u_2\}$. Let the fairness constraints be given by the temporal weight demands $\underline{w}_1 = \underline{w}_2 = 0.6$ and $\bar{w}_1 = \bar{w}_2 = 1$. This requires each user to be activated for at least 0.6 fraction of the time. One possible scheduling strategy in this scenario is the Weighted Round Robin (WRR) strategy shown in Figure 1(b). The strategy is described below:

$$Q_t = \begin{cases} v_1, & \text{if } 0 \leq \text{mod}_{10}(t) \leq 2, \\ v_2, & \text{if } 3 \leq \text{mod}_{10}(t) \leq 5, \\ v_{1,2}, & \text{if } 6 \leq \text{mod}_{10}(t) \leq 9. \end{cases} \quad (9)$$

The WRR strategy is a non-opportunistic strategy where virtual users are chosen independently of the realization of the performance vector. As a result, the temporal share $A_{i,t}^Q, i \in [n], t \in \mathbb{N}$ is a deterministic function of t . Note that $\underline{A}_i^Q = 0.3 + 0.4 = 0.7, i = 1, 2$; hence the WRR strategy satisfies the temporal demand conditions (4). Also, it is straightforward to show that the average network utility is $U^Q = 0.3\mathbb{E}(R_1) + 0.3\mathbb{E}(R_2) + 0.4\mathbb{E}(R_3)$.

The scheduler $Q = (Q_t)_{t \in \mathbb{N}}$ takes the matrix $R^{m \times t}$ of performance values up to time t as input and outputs the virtual user $v_j, j \in [m]$ which is to be activated at time t . Temporal share $A_{i,t}^Q, i \in [n], t \in \mathbb{N}$ in (5) represents the fraction of time-slots in which user u_i is activated until time t . The variable $\underline{A}_i^Q, i \in [n]$ is an asymptotic lower bound to the temporal share of user u_i

and (4) represents the temporal fairness constraints. Furthermore, U_t^Q and U^Q are the instantaneous and average system utilities, respectively. The objective is to design a scheduling strategy which achieves the maximum average network utility while satisfying temporal fairness constraints.

Definition 6 (Optimal Strategy): For the scheduling setup parametrized by $(n, N_{\max}, \underline{w}^n, \bar{w}^n, f_{R^m})$, a strategy Q^* is optimal if and only if

$$Q^* \in \operatorname{argmax}_{Q \in \mathcal{Q}} U^Q, \quad (10)$$

where \mathcal{Q} is the set of all strategies for the scheduling setup.

The set \mathcal{Q} includes strategies with memory as well as non-stationary and stochastic strategies. As a result, the cardinality of the set is large and the optimization problem described in Equation (10) is not computable through exhaustive search. However, in Section IV we show that this optimization problem can be expressed in a computable form by restricting the search to a specific subset of stationary and memoryless strategies called *threshold based strategies*. More precisely, we show that any optimal strategy is equivalent to a threshold based strategy where equivalence between strategies defined below

Definition 7 (Equivalence): For the scheduling setup $(n, N_{\max}, \underline{w}^n, \bar{w}^n, f_{R^m})$ two strategies Q and Q' are called equivalent ($Q \sim Q'$) if:

$$\lim_{t \rightarrow \infty} \frac{1}{t} \sum_{k=1}^t P(Q_k(R^{m \times k}) = Q'_k(R^{m \times k})) = 1.$$

Definition 8 (Stationary and Memoryless): A strategy $Q = (Q_t)_{t \in \mathbb{N}}$ is called memoryless if $Q_t(R^{m \times t}), t \in \mathbb{N}$ is only a function of the performance vector $(R_{1,t}, R_{2,t}, \dots, R_{m,t})$ corresponding to time t . For the memoryless strategy Q , we write $Q_t(R^m)$ instead of $Q_t(R^{m \times t})$ when there is no ambiguity. A memoryless strategy is called stationary if $Q_t(R^m) = Q_{t'}(R^m)$ for any $t, t' \in \mathbb{N}$.

Lemma 1: For a memoryless and stationary strategy Q , the following limits exist:

$$A_i^Q = \lim_{t \rightarrow \infty} A_{i,t}^Q, \quad U^Q = \lim_{t \rightarrow \infty} U_t^Q. \quad (11)$$

The proof is provided in the Appendix.

Definition 9 (TBS): For the scheduling setup $(n, N_{\max}, \underline{w}^n, \bar{w}^n, f_{R^m})$ a threshold based strategy (TBS) is characterized by the vector $\lambda^n \in \mathbb{R}^n$. The strategy $Q_{TBS}(\lambda^n) = (Q_{TBS,t})_{t \in \mathbb{N}}$ is defined as:

$$Q_{TBS,t}(R^{m \times t}) = \operatorname{argmax}_{v_j \in \mathcal{V}} S(v_j, R_{j,t}), \quad t \in \mathbb{N}, \quad (12)$$

where $S(v_j, R_{j,t}) = R_{j,t} + \sum_{i=1}^n \lambda_i \mathbb{1}_{\{u_i \in v_j\}}$ is the ‘scheduling measure’ corresponding to the virtual user v_j . The resulting temporal shares are represented as $w_i = A_i^{Q_{TBS}}, i \in [n]$. The utility of the TBS is written as $U_{w^n}(\lambda^n)$. The space of all threshold based strategies is denoted by \mathcal{Q}_{TBS} .

We note that threshold based strategies are stationary and memoryless. The reason is that the output of $Q_{TBS,t}, t \in \mathbb{N}$ in (12) depends only on the threshold vector λ^n and the realization of R^m at time t .

Example 2: Consider the NOMA system described in Example 1. A TBS with threshold vector $\lambda^2 = (\lambda_1, \lambda_2)$ has the following scheduling measures:

$$\begin{aligned} S(\mathcal{V}_1, R_{1,t}) &= R_{1,t} + \lambda_1, \\ S(\mathcal{V}_2, R_{2,t}) &= R_{2,t} + \lambda_2, \\ S(\mathcal{V}_{1,2}, R_{1,2,t}) &= R_{1,2,t} + \lambda_1 + \lambda_2. \end{aligned}$$

The virtual user with the highest scheduling measure is chosen at each time-slot. Note that the probability of a tie among the scheduling measures is 0 since the performance vector R^m is assumed to be jointly continuous.

IV. EXISTENCE OF OPTIMAL THRESHOLD BASED STRATEGIES

In this section, we show that for any scheduling problem with temporal fairness constraints, optimal utility can be achieved using a threshold based scheduling strategy. Therefore, in considering the optimization problem described in Equation (10), the set of strategies \mathcal{Q} can be restricted to the set of threshold based strategies. Furthermore, we show that any scheduling strategy which achieves optimal utility is equivalent to a threshold based strategy, where equivalence between strategies is defined in Definition 7.

A. Optimal Temporally Fair NOMA Scheduling

Theorem 1: For the NOMA scheduling setup $(n, N_{\max}, \underline{w}^n, \bar{w}^n, f_{R^m})$, assume that $\mathcal{Q} \neq \emptyset$. Then, there exists an optimal threshold based strategy Q_{TBS} . Furthermore, for any optimal strategy Q , there exists a threshold based strategy Q' such that $Q \sim Q'$.

The condition $\mathcal{Q} \neq \emptyset$ in Theorem 1 is called the feasibility condition and is investigated in Section IV-B. The proof of the theorem follows from the following steps:

- Under equality temporal demand constraints where $\underline{w}^n = \bar{w}^n = w^n$, existence of optimal TBSs follows from a generalization of the intermediate value theorem called the Poincaré-Miranda Theorem [34].
- The uniqueness of an optimal strategy up to equivalence follows from a variant of the dual (Lagrangian multiplier) optimization method.
- Under inequality temporal demand constraints, the proof of existence follows by discretizing the feasible space and solving the optimization for each point on the discretized space under equality constraints.

The complete proof of Theorem 1 is provided in the Appendix. The following corollaries follow from the proof.

Corollary 1: Consider the NOMA scheduling setup under equality temporal demand constraints $(n, N_{\max}, w^n, w^n, f_{R^m})$, where $\mathcal{Q} \neq \emptyset$. There exists a unique TBS Q_{TBS} satisfying the temporal demand constraints and this TBS is the optimal scheduling strategy for this setup.

The following corollary states that the search for the optimal strategy in Equation (10) may be restricted to the set of TBSs.

Corollary 2: For the scheduling setup $(n, N_{\max}, \underline{w}^n, \bar{w}^n, f_{R^m})$, the optimal achievable utility is given by:

$$U_{\underline{w}^n, \bar{w}^n}^* \triangleq \max_{\lambda^n: \underline{w}_i \leq A_i^{Q_{TBS}} \leq \bar{w}_i} U_{w^n}(\lambda^n), \quad (13)$$

where $U_{w^n}(\lambda^n)$ is defined in Definition 9.

As a consequence of Theorem 1, under equality temporal demand constraints, the optimal achievable utility is equal to the utility of the unique TBS satisfying the temporal demand constraints (i.e. $U_{w^n, w^n}^* = U_{w^n}(\lambda^n)$). The reason is that the threshold based strategy achieves optimal utility among all strategies with temporal shares equal to w^n .

The following Corollary is used in Section VII to provide a low complexity algorithm for constructing optimal TBSs.

Corollary 3: For the NOMA scheduling setup $(n, N_{\max}, \underline{w}^n, \bar{w}^n, f_{R^m})$, assume that there exist positive thresholds $\lambda_1, \lambda_2, \dots, \lambda_n$ satisfying the complimentary slackness conditions:

$$\begin{aligned} \lambda_i \left(A_i^{Q_{TBS}} - \underline{w}_i \right) &= 0, \forall i \in [n], \\ \underline{w}_i &\leq A_i^{Q_{TBS}} \leq \bar{w}_i, \forall i \in [n], \end{aligned}$$

where Q_{TBS} is the TBS corresponding to the threshold vector λ^n . Then, Q_{TBS} is an optimal scheduling strategy.

Note that the complementary slackness conditions in Corollary 3 are written only in terms of the lower temporal demands. Similar sufficient conditions can be derived in terms of the upper temporal share demands.

Remark 4: If $Q \sim Q'$, then the two scheduling strategies activate the same subsets of users in almost all time-slots. As a result, the two strategies have the same performance under any long-term fairness and utility criteria. Let \mathcal{Q}^* be the set of all optimality achieving strategies under temporal demand constraints. A consequence of Theorem 1 is that all of the strategies in \mathcal{Q}^* have the same performance with each other under any additional utility or fairness criteria.

B. Feasible Temporal Share Region

Section IV-A affirms the existence of a TBS that achieves the optimal average system utility given that the temporal demands are feasible. However, some values of $(\underline{w}^n, \bar{w}^n)$, are not achievable by any scheduling strategy. In other words, the set \mathcal{Q} is empty for certain pairs of constraint vectors $(\underline{w}^n, \bar{w}^n)$. In this section, we provide a variable elimination method which allows us to characterize the feasible region for a given scheduling setup as a function of its temporal demand vectors.

Definition 10: A scheduling setup $(n, N_{\max}, \underline{w}^n, \bar{w}^n, f_{R^m})$ is called feasible if $\mathcal{Q} \neq \emptyset$. The set of temporal shares w^n for which the setup is feasible under equality constraints is called the feasible region and is denoted by \mathcal{W} .

The following theorem characterizes the set of all feasible scheduling setups.

Theorem 2: A scheduling setup with equality temporal constraints $(n, N_{\max}, w^n, w^n, f_{R^m})$ is feasible if and only if there exist a set of non-negative values $\{a_j : j \in [m]\}$ satisfying the

following bounds:

$$\sum_{j \in [m]} a_j = 1, \quad \sum_{j: u_i \in \mathcal{V}_j} a_j = w_i, \quad \forall i \in [n], \quad 0 \leq a_j, \quad \forall j \in [m]. \quad (14)$$

Furthermore, the scheduling setup with inequality temporal constraints $(n, N_{\max}, \underline{w}^n, \bar{w}^n, f_{R^m})$ is feasible if and only if there exist a set of non-negative numbers $\{w_i : i \in [n]\}$. Such that i) $(n, N_{\max}, w^n, w^n, f_{R^m})$ is feasible, and ii) the following bounds are satisfied:

$$\forall i \in [n] : \underline{w}_i \leq w_i \leq \bar{w}_i.$$

Proof Sketch: In order to prove that $\mathcal{Q} \neq \emptyset$ under equality constraints, we use a WRR scheduler in which the weight assigned to \mathcal{V}_j is equal to a_j . Under inequality temporal constraints, in order to have $\mathcal{Q} \neq \emptyset$, it suffices that there is a vector of temporal shares in the feasible region which satisfies the inequality constraints. On the other hand, if the scheduling setup is feasible (i.e. $\mathcal{Q} \neq \emptyset$), then a WRR strategy exists which satisfies the temporal demand constraints. Taking a_j to be equal to the temporal weight assigned to \mathcal{V}_j , it is straightforward to verify that Equations in (14) hold. ■

The feasibility conditions in Theorem 2 are written in terms of auxiliary variables $a_j, j \in [m]$ which can be interpreted as the temporal shares of the virtual users. However, it is often desirable to write the feasibility conditions in terms of the temporal share vector w^n . The conditions can be re-written in the desired form using the Fourier-Motzkin elimination (FME) algorithm. The standard FME algorithm has worst case computational complexity of order $O(m^{2^m - n - 1})$ [35]. In [36], a method for variable elimination was proposed which has a significantly lower computation complexity. The method leads to the following algorithm for determining the feasible region:

Step 1: Eliminate $a_i, i \leq n + 1$ using the equality constraints (14):

$$a_i = w_i - \sum_{j: u_i \in \mathcal{V}_j} a_j, \quad i \in [n], \quad a_{n+1} = 1 - \sum_{j \in [m], j \neq n+1} a_j.$$

That is, replace $a_i, i \leq n + 1$ in all inequality constraints (14) by the right hand sides in the above equations.

Step 2: Define $c_{l,j}, l \in [m], 1 \leq j \leq n$ as the coefficient of w_j in the l th inequality after Step 1. Also, define $c_{l,j}, l \in [m], n + 2 \leq j \leq m$ as the coefficient of a_j in the l th inequality. Construct the dual system of equations:

$$\sum_{l \in [m]} c_{l,j} x_l = 0, \quad x_l \in \mathbb{N} \cup \{0\}, \quad j \in \{n + 2, n + 3, \dots, m\}.$$

Step 3: Use the Normaliz algorithm [37] to find the Hilbert basis for the solution space of the dual system. Let $\mathcal{B} = \{b_1^m, b_2^m, \dots, b_k^m\}$ be the Hilbert basis, where k is the number of Hilbert basis elements.

Step 4: Let $b_i^m = (b_{i,1}, b_{i,2}, \dots, b_{i,m}), i \in [k]$. The following system of inequalities gives the feasible region:

$$0 \leq \sum_{l \in [n+1]} \sum_{j \in [n]} b_{i,l} c_{j,l} w_j, \quad i \in [k]. \quad (15)$$

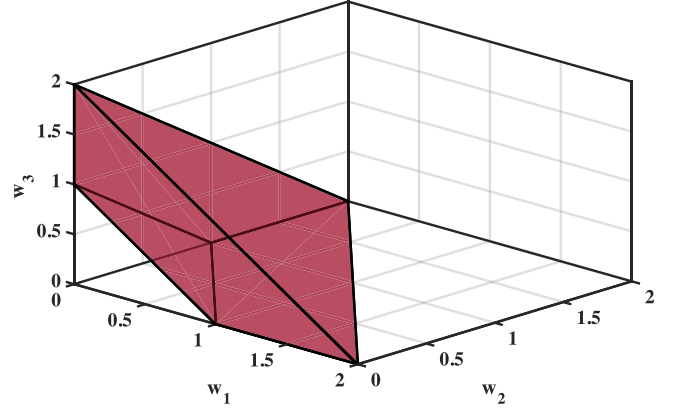


Fig. 2. The colored region shows the set of feasible weight vectors for the three user NOMA problem with $N_{\max} = 2$.

The elimination process is explained in the following example.

Example 3: Consider a three user downlink NOMA scenario with $N_{\max} = 2$. The scheduling setup is feasible if there exists a vector of virtual user temporal weights $(a_1, a_2, a_3, a_{1,2}, a_{1,3}, a_{2,3})$ such that:

$$\begin{aligned} 0 &\leq a_1, \quad 0 \leq a_2, \quad 0 \leq a_3, \quad 0 \leq a_{1,2}, \quad 0 \leq a_{1,3}, \quad 0 \leq a_{2,3} \\ a_1 + a_2 + a_3 + a_{1,2} + a_{1,3} + a_{2,3} &= 1, \\ a_1 + a_{1,2} + a_{1,3} = w_1, \quad a_2 + a_{1,2} + a_{2,3} &= w_2, \\ a_3 + a_{1,3} + a_{2,3} &= w_3. \end{aligned}$$

Using the equality constraints, one could write a_1, a_2, a_3 and $a_{1,2}$ as functions of $w_1, w_2, w_3, a_{1,3}$ and $a_{2,3}$. We get:

$$\begin{aligned} 0 &\leq 1 + a_{1,3} - w_1 - w_3, \quad 0 \leq 1 + a_{2,3} - w_2 - w_3, \\ a_{1,3} + a_{2,3} &\leq \min(w_3, w_1 + w_2 + w_3 - 1), \\ 0 &\leq a_{1,3}, \quad 0 \leq a_{2,3}. \end{aligned}$$

There are a total of five inequalities, i.e. $k = 5$. The dual system is given by:

$$x_1 - x_3 + x_4 = 0, \quad x_2 - x_3 + x_5 = 0.$$

The Hilbert basis is $\mathcal{B} = \{(1, 1, 1, 0, 0), (0, 0, 1, 1, 1), (0, 1, 1, 1, 0), (1, 0, 1, 0, 1)\}$. From Equation (15), the feasible region is as follows:

$$0 \leq w_i \leq 1, \quad i \in [3], \quad 1 \leq w_1 + w_2 + w_3 \leq 2.$$

The region is shown in Figure 2. The figure can be interpreted as follows: the sum of the temporal shares of all users cannot exceed two since no more than two users can be activated at each time-slot. Furthermore, the sum cannot be lower than one since at least one user is activated at each time-slot.

The problem of determining the feasible region is more complicated for large non-homogeneous NOMA systems where specific subsets of users cannot be activated simultaneously due to practical considerations. In such instances the elimination method proposed in this section can be a valuable tool in determining the feasible region.

V. CONSTRUCTION OF OPTIMAL SCHEDULING STRATEGIES

In the previous section, it was shown that for any feasible scheduling problem, optimal utility is achieved using TBSs. In this section, we address the construction of optimal scheduling strategies and provide an iterative method which builds upon the Robbins-Monro algorithm [38] to find optimal thresholds for TBSs. Note that the scheduler does not have access to the statistics of the performance vector. The algorithm proposed in this section uses the empirical observations of the realizations of the performance vector to find the optimal thresholds iteratively.

A. The Robbins-Monro Algorithm

The Robbins-Monro algorithm [38] is a method for finding the roots of the univariate function $f : \mathbb{R} \rightarrow \mathbb{R}$ based on a limited number of noisy samples of $f(x)$, $x \in \mathbb{R}$. More precisely, assume that we take l noisy samples $g_t = f(x_t) + \epsilon_t$ of the function $f(\cdot)$ at x_t , $t \in [l]$, where the random variable ϵ_t is the sampling noise at time t and l is a fixed natural number.

The objective is to approximate the solution of $f(x) = 0$ by choosing $x_t, t \in [l]$ suitably such that the approximation converges to the root as $l \rightarrow \infty$. The algorithm was extended to find roots of multi-variate functions by Ruppert [39]. Let $f : \mathbb{R}^n \rightarrow \mathbb{R}^n$ be a mapping of the n -dimensional Euclidean space onto itself. Let $g_t = f(x_t^n) + \epsilon_t^n$ be the noisy sample of $f(x_t^n)$ at $x_t^n, t \in [l]$, and the step-size sequence $(s_t)_{t \in \mathbb{N}}$ be a sequence of positive real numbers. It can be shown that sequence $x_{t+1}^n = x_t^n - s_t g_t^n$ converges to the solution of the system $f(x^n) = 0$ if the following conditions hold:

- 1) *Solvability*: The function $f(\cdot)$ has a root x^{*n} .
- 2) *Local Monotonicity*: $(x^n - x^{*n})^T f(x^n) > 0$ for $x^n \neq x^{*n}$.
- 3) *Zero-mean and i.i.d. noise*: $\epsilon_t^n, t \in \mathbb{N}$ is an i.i.d. sequence and $\mathbb{E}(\epsilon_t^n) = 0$.
- 4) *Step-size constraints*: $s_t > 0$, $\lim_{t \rightarrow \infty} s_t = 0$, $\sum_{t=1}^{\infty} s_t = \infty$, $\sum_{t=1}^{\infty} s_t^2 < \infty$.

B. Finding Thresholds under Equality Constraints

In Corollary 1, we showed that any threshold based strategy satisfying the equality temporal constraints is optimal. As a result, the objective of finding the optimal scheduling strategy is reduced to finding the thresholds which lead to a TBS satisfying the temporal demand constraints. More precisely, we are interested in finding the threshold vector λ^n such that

$$A_i^{Q_{TBS}(\lambda^n)} = w_i, i \in [n]. \quad (16)$$

Hence, finding the optimal TBS is equivalent to solving the non-linear system of equations in (16). Next, we show that the empirical observation of the realizations of R^m at the BS is sufficient to find the optimal thresholds using the multi-variate version of the Robbins-Monro stochastic approximation method [39].

In the scheduling problem, consider $f_i(\lambda^n) = A_i^Q(\lambda^n) - w_i, i \in [n]$. We are interested in finding the root of the function $f(\cdot)$ provided that the root exists (i.e. $\mathcal{Q} \neq \emptyset$). In Theorem 3, we show that conditions (1)-(4) provided above are

satisfied for a suitable step-size sequence. Note that $A_i^Q(\lambda^n)$ depends on the statistics of the performance vector R^m and is not explicitly available in practice. Assume that at time t , the scheduler uses the threshold vector λ_t^n . Then, it observes $g_{t,i} \triangleq \mathbb{1}\{u_i \in Q_t(\lambda_t^n)\} - w_i$ which is a noisy sample of $f(\lambda_t^n) = A_i^Q(\lambda_t^n) - w_i$. The sampling noise is $\epsilon_{t,i} = g_{t,i}(\lambda_t^n) - f_i(\lambda_t^n) = \mathbb{1}\{u_i \in Q_t(\lambda_t^n)\} - A_i^Q(\lambda_t^n)$. The sequence of sampling noise vectors $\epsilon_t^n, t \in \mathbb{N}$ is an i.i.d. sequence since $Q_t(\lambda_t^n)$ depends only on the realization of R^m at time t which are assumed to be i.i.d. over time. Furthermore, it is straightforward to show that $\mathbb{E}(\epsilon_{t,i}) = 0$. Therefore, conditions (1) and (3) are satisfied. The following theorem shows that conditions (2) and (4) hold for $N_{\max} > 1$.

Theorem 3: Let $f_i(\lambda^n) = A_i^Q(\lambda^n) - w_i, i \in [n]$. The convergence conditions (1)-(4) in the multi-variate Robbins-Monro algorithm are satisfied for step-size the sequence $s_t = \frac{1}{t}, t \in \mathbb{N}$.

The proof is provided in the Appendix.

C. Finding Thresholds Under General Temporal Constraints

In this section, we provide an algorithm for finding the optimal TBS thresholds under general temporal demand constraints (Algorithm 1). The optimization algorithm uses a combination of the gradient projection method [40] and the Robbins-Monro algorithm described in the previous section. The algorithm leverages the concavity of $U_{\underline{w}^n, \bar{w}^n}^*$ shown in Lemma 2 and applies gradient projection to ensure that the solution converges to an optimal threshold vector within the feasible space. Furthermore, we build upon Algorithm 1 to propose a low-complexity heuristic algorithm (Algorithm 2) which is used in Section VII for simulations.

Lemma 2: The optimal achievable utility $U_{\underline{w}^n, \bar{w}^n}^*$ is jointly concave as a function of $(\underline{w}^n, \bar{w}^n)$.

The proof is provided in the Appendix. As a consequence of Lemma 2, the optimization in (13) can be performed using standard gradient projection methods [40]. Note that the gradient projection method requires prior knowledge of the feasible set which is characterized using the method in Section IV-B.

Algorithm 1 performs an iterative two-step optimization. At each iteration, in the first step, given a fixed temporal demand vector w^n , the Robbins-Monro algorithm is used to find the thresholds under equality temporal constraints. Next, the gradient projection method is used to update the weight vector w^n based on $\nabla U_{w^n, w^n}$. The algorithm converges to the optimal utility due to the concavity of $U_{\underline{w}^n, \bar{w}^n}^*$. The iteration stops if $\Delta \geq \epsilon$, where Δ represents the variation in w^n at each step and ϵ is the stopping parameter. It can be noted that the choice of the initial demand vector w_0^n does not affect the convergence of the proposed method since U_{w^n, w^n}^* is jointly concave as shown in Lemma 2.

Algorithm 1 requires estimating the gradient of U_{w^n, w^n}^* which entails high computational complexity. To elaborate, in order to use the gradient projection method, the scheduler needs to know $\nabla U_{w^n, w^n}^*$. However, the scheduler does not know the statistics of the performance vector. As a result, it must estimate $\nabla U_{w^n, w^n}^*$ using a gradient estimation method based on the empirical observations of the performance vector. As an alternative, we propose

Algorithm 1: Two-stage Threshold Optimization in TBS.

- 1: Obtain feasibility region \mathcal{W} (Section IV-B).
 - 2: Set $\epsilon > 0$ and $\Delta = 2\epsilon$.
 - 3: Choose initial demand vector $w^n = w_0^n$.
 - 4: **while** $\Delta \geq \epsilon$ **do**
 - 5: Find U_{w^n, w^n}^* and corresponding λ^n (Robbins-Monro Algorithm in Section V-B).
 - 6: Update w^n based on $\nabla U_{w^n, w^n}^*$ (gradient projection step).
 - 7: $\Delta = \|w_{new}^n - w^n\|$
 - 8: **end while**
-

Algorithm 2: Heuristic Threshold Optimization in TBS.

Initialization: $\lambda_{1,i} = 0, i \in [n]$

- 1: **for** $t \in \mathbb{N}$ **do**
 - 2: $\mathcal{V}_t = Q_t(\lambda_t^n)$
 - 3: $A_{t+1,i}^Q = A_{t,i}^Q + \frac{1}{t+1} (\mathbb{1}\{i \in \mathcal{V}_t\} - A_{t,i}^Q)$
 - 4: $\lambda_{\min} = \min_{i \in [n]} \lambda_{t,i}$
 - 5: $\lambda_{t+1,i} =$
 $\lambda_{t,i} - s (\lambda_{t,i} - \lambda_{\min}) (\mathbb{1}\{u_i \in \mathcal{V}_t\} - \underline{w}_i), i \in [n]$
 - 6: **for** $i = 1$ to n **do**
 - 7: **if** $\lambda_{t,i} = \lambda_{\min}$ and $A_{t+1,i}^Q < \underline{w}_i$ **then**
 - 8: $\lambda_{t+1,i} = \lambda_{t,i} + s (\underline{w}_i - A_{t+1,i}^Q)$
 - 9: **end if**
 - 10: **if** $\lambda_{t,i} = \lambda_{\min}$ and $\lambda_{\min} < 0$ **then**
 - 11: $\lambda_{t+1,i} = \lambda_{t,i} + s$
 - 12: **end if**
 - 13: **end for**
 - 14: **end for**
-

Algorithm 2 which is a low complexity heuristic variation of Algorithm 1. The algorithm is constructed using the complementary slackness conditions provided in Corollary 3. Algorithm 2 replaces gradient projection in Algorithm 1 by a simple perturbation step.

Algorithm 2 starts with a vector of initial thresholds. At time-slot t , it chooses virtual user \mathcal{V}_t to be activated based on the threshold vector λ_t^n . It updates the temporal shares and thresholds based on the scheduling decision at the end of the time-slot (line 2–5). The update rule for the thresholds given in line 5 is a variation of the Robbins-Monro update described in Section V. The parameter s is the step-size. Lines (6–13) replace the gradient projection step in Algorithm 1 and verify that the temporal demand constraints and dual feasibility conditions are satisfied. The computational complexity of the algorithm grows polynomially in the number of users. For instance, when $N_{\max} = 2$, the computational complexity at each time-slot is proportional to the number of virtual users and is $O(n^2)$.

VI. DISCRETE AND MIXED PERFORMANCE VARIABLES

So far, we have assumed that the performance vector R^m is jointly continuous. The proofs provided for Theorems 1 and 3 rely on the joint continuity assumption. However, in practical scenarios, the performance vector is a vector of discrete or

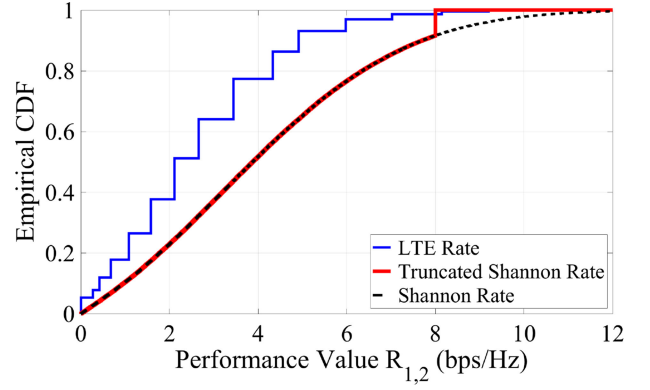


Fig. 3. Empirical CDF of performance value of virtual user $\mathcal{V}_{1,2}$ in two user NOMA.

mixed random variables. For instance, in cellular systems, the performance vector is discrete due to discrete modulation and coding schemes.

The performance value of a virtual user is a function of the SINR of its elements. For instance, in Section III, sum-rate in the NOMA downlink scenario was considered as the performance metric which is a logarithmic function of the SINRs. Since the logarithm function is continuous, the performance vector is a jointly continuous vector of random variables. However, in practical scenarios, the function which relates the SINR to the performance value is neither injective nor continuous. The function is determined by the choice of the modulation and coding schemes at each time-slot. Moreover, in some applications, the performance value is approximated by a truncated Shannon rate function, i.e. $R = \min\{\log_2(1 + \text{SINR}), \gamma_{\max}\}$, where γ_{\max} is the maximum data rate supported by the system. In this case, the performance value has a mixed distribution function. Figure 3 shows the empirical CDF of the performance value of virtual user $\mathcal{V}_{1,2}$ in the downlink of a two user NOMA system with SIC, where the performance value is taken as i) the Shannon sum-rate for NOMA downlink scenario as described in Section III, ii) truncated Shannon sum-rate, and iii) sum-rate with LTE modulation and coding schemes. In the truncated Shannon sum-rate model we use $\gamma_{\max} = 4$ bps/Hz and in the LTE rate model we use the parameters in [41, Table 7.2.3-1], where 15 combinations of modulation and coding schemes are used.

The analysis provided in the previous sections cannot be applied directly to mixed and discrete performance vectors. The reason is that when the performance values are jointly continuous, the probability of having a tie among the scheduling measures in a TBS is zero. However, there may be more than one virtual user with the highest scheduling measure in the case of a mixed or discrete performance vector. In such scenarios, there is a need for a tie-breaking rule which affects the optimality of the scheduler. One widely used solution in OMA scheduling is to use a stochastic tie-breaker where in the event of a tie, one of the users is activated randomly based on a given probability distribution called the tie-breaking probability [19]. This requires a joint optimization of the thresholds and the tie-breaking rule.

We propose a new class of scheduling strategies called ℓ -perturbed TBSs to handle mixed and discrete random variables. An ℓ -perturbed TBS is a variation of TBSs where the scheduling measure takes a perturbation of the performance vector as its input. To elaborate, fix $\ell \in \mathbb{N}$. Define $\tilde{R}_{j,t}(\ell) = R_{j,t} + N_{j,t,1/\ell}$, $j \in [m]$ where $N_{j,t,1/\ell} \sim \text{Unif}[-1/\ell, 1/\ell]$ and the variables $N_{j,t,1/\ell}$ are jointly independent. It is straightforward to show that $(\tilde{R}_{j,t}(\ell))_{j \in [m]}$ is a jointly continuous vector of random variables. Let Q be a TBS characterized by the threshold vector λ^n . At time-slot t , the ℓ -perturbed TBS $Q_{1/\ell}$ activates $\mathcal{V}_{J,t} = Q_{1/\ell}(R^{m \times t}) = Q(\tilde{R}^{m \times t})$, where J is the random variable corresponding to the index of the activated virtual user. The resulting utility is equal to $R_{J,t}$. The class of perturbed TBSs are formally defined below.

Definition 11 (Discrete Scheduling Setup): A discrete scheduling setup is characterized by $(n, N_{\max}, \underline{w}^n, \bar{w}^n, R^m)$, where R^m may be a discrete or mixed vector of random variables.

Definition 12 (ℓ -PTBS): For the scheduling setup $(n, N_{\max}, \underline{w}^n, \bar{w}^n, R^m)$ an ℓ -perturbed threshold based strategy (ℓ -PTBS) is characterized by the vector $\lambda^n \in \mathbb{R}^n$. The strategy $Q_{1/\ell}(\lambda^n) = (Q_{1/\ell,t})_{t \in \mathbb{N}}$ is defined as:

$$Q_{1/\ell,t}(R^{m \times t}) = \operatorname{argmax}_{\mathcal{V}_j} S_\ell(\mathcal{V}_j, \tilde{R}_{j,t}), \quad t \in \mathbb{N}, \quad (17)$$

where $\tilde{R}_{j,t}(\ell) = R_{j,t} + N_{j,t,1/\ell}$ are the perturbed performance values and $N_{j,t,1/\ell} \sim \text{Unif}[-1/\ell, 1/\ell]$ are jointly independent.

The following theorem shows that the average system utility for the designed ℓ -PTBS approaches the optimal utility of the original system as $\ell \rightarrow \infty$. However, it should be noted that the precision supported by the scheduler's equipment sets an upper limit on ℓ .

Theorem 4: Let Q^* be the optimal scheduling strategy for the setup $\Omega_0 = (n, N_{\max}, \underline{w}^n, \bar{w}^n, R^m)$. Let $Q_{1/\ell}^*$ be the optimal TBS for the setup $\Omega_{1/\ell} = (n, N_{\max}, \underline{w}^n, \bar{w}^n, f_{\tilde{R}^m}^m)$, where $\tilde{R}^m = R^m + N_{1/\ell}^m$ and $N_{1/\ell}^m$ is a vector of independent $\text{Unif}[-1/\ell, 1/\ell]$ variables. Let $\hat{Q}_{1/\ell}$ be the ℓ -PTBS characterized by the same threshold vector as $Q_{1/\ell}^*$. Define U^* and $U_{1/\ell}$ as the average system utility due to Q^* and $\hat{Q}_{1/\ell}$ when applied to system Ω_0 , respectively. Then,

$$\lim_{\ell \rightarrow \infty} (U^* - U_{1/\ell}) = 0,$$

where convergence is in probability. Alternatively, the utility of $\hat{Q}_{1/\ell}$ applied to Ω_0 converges to the optimal utility as $\ell \rightarrow \infty$.

The proof is provided in Appendix E.

VII. NUMERICAL RESULTS AND SIMULATIONS

In this section, we provide various numerical examples and simulations to evaluate the performance of the approaches proposed in Sections V and VI. We simulate the DL of a small-cell NOMA system consisting of a BS and a number of users distributed uniformly at random in a ring around the BS with inner and outer radii of 20 m and 100 m, respectively. Two user mobility models are considered in the simulations. In the first model, the users are assumed to be static, whereas the second model

TABLE I
SIMULATION PARAMETERS

Parameter	Value
Scenario	NOMA downlink with SIC
Number of users	2, 3, 4, 5, 6
Cell radius	100 m
System Bandwidth	10 MHz
Number of time-slots	5×10^6
Maximum spectral efficiency	6 bps/Hz
Noise spectral density	-174 dBm/Hz
Noise figure	9 dB
Shadowing standard deviation	8 dB
Path loss in dB	$128.1 + 37.6 \log_{10}(d \text{ in km})$
Rate in bps/Hz	$\min\{\log_2(1 + \text{SINR}), 6\}$
User mobility models	Static, 2D random walk

uses a two-dimensional random walk. Table I lists the network parameters. We consider $N_{\max} = 2$, i.e. an individual user or a pair of users is scheduled at each time-slot. We assume that there are no upper temporal demand constraints. The user SINRs are modeled as described in Equation (1) and the network utility is assumed to be truncated Shannon sum-rate unless otherwise stated. At each time-slot prior to scheduling, a max-min power optimization is performed for each virtual user [11]. For a given virtual user, we find the transmit power which maximizes the minimum individual user rates in that virtual user. This max-min optimization allows for a balanced rate allocation within the virtual user. It can be shown that the max-min optimization is quasi-concave. Consequently, quasi-concave programming methods such as bisection search can be used to find the optimal transmit powers [11]. Maximum BS transmit power constraint is chosen such that the average SNR of 10 dB is achievable when a single user is active on the boundary of the cell. We use Algorithm 2 described in Section V for simulations. The step-size s is taken to be 0.001.

A. Performance Evaluation

We evaluate the performance of the NOMA scheduler in a scenario where the users are static. As a benchmark, we consider an OMA system where a single user is activated at each time-slot. To find a temporal fair scheduler in an OMA system, we consider the setup when $N_{\max} = 1$. We also consider Round Robin (RR) scheduling as another benchmark. Figure 4 shows the empirical cumulative distribution function (CDF) of the network throughput in a network with $n = 5$ users and $\underline{w}_i = 0.2, \forall i \in [5]$ for various scheduling strategies. We observe that there are significant improvements in terms of network throughput when the TBS (labeled opportunistic NOMA) is used compared to OMA (labeled opportunistic OMA) as expected. Furthermore, we note that RR scheduling in NOMA leads to a significant performance loss. The RR strategy chooses the virtual user regardless of the performance in that time-slot. As a result, the strategy is particularly inefficient in NOMA systems. The reason is that SIC which is used in NOMA may have a poor performance for a given virtual user in some time-slots.

Table II lists the percentage of the average throughput gain when using opportunistic NOMA scheduler compared to an opportunistic OMA scheduler. For a given number of users

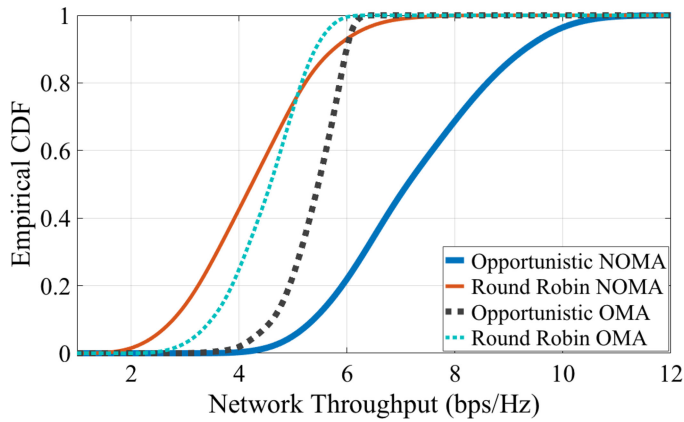


Fig. 4. Empirical CDF of network throughput for NOMA and OMA systems using different scheduling schemes when the users are static.

TABLE II
AVERAGE THROUGHPUT GAIN OF OPPORTUNISTIC NOMA SCHEDULING OVER OPPORTUNISTIC OMA SCHEDULING

Number of users	2	3	4	5	6
Throughput gain (%)	7.33	18.99	27.08	37.14	45.47

$n \in \{2, 3, \dots, 6\}$, we simulated 100 independent realizations of the network. It can be observed that increasing the number of users boosts the NOMA performance gain. This is due to the fact that the number of virtual users increases as n becomes larger. As a result, the NOMA scheduler has more options in the choice of the active virtual user.

B. Convergence

In this section, we investigate the evolution of the scheduling thresholds when running Algorithm 2. We consider a scenario with $n = 5$ users and $\underline{w}^5 = [0.1, 0.1, 0.4, 0.3, 0.1]$. We assume that the users are static. Figure 5(a) shows the long-term user temporal shares $A_Q^i, t \in [5]$ and the user thresholds. It can be seen that the temporal demand constraints are satisfied. Also, the thresholds satisfy the optimality conditions discussed in Corollary 3. Figure 5(b) shows the evolution of the thresholds in different iterations of Algorithm 2.

In Figure 6, we consider the previous scenario with mobile users. We model the mobility of the users by a two-dimensional random walk where each user takes one step per time-slot in a direction θ uniformly distributed in $[0, 2\pi]$. Furthermore, we assume that the speed of the user at each step is randomly distributed between 1 m/s and 10 m/s. It is also assumed that the users do not exit the cell. In this scenario, the performance vector R^m is not stationary and $A_i^Q(\lambda^n)$ is time-varying. Therefore, the optimal thresholds change over time. Figure 6(a) shows the long-term temporal share of the users and the evolution of the thresholds in time. It can be seen that the thresholds track the variation of the system and the desired temporal demand constraints are satisfied. Figure 6(b) shows the evolution of the users' thresholds as the iterative algorithm proceeds. It can be observed that

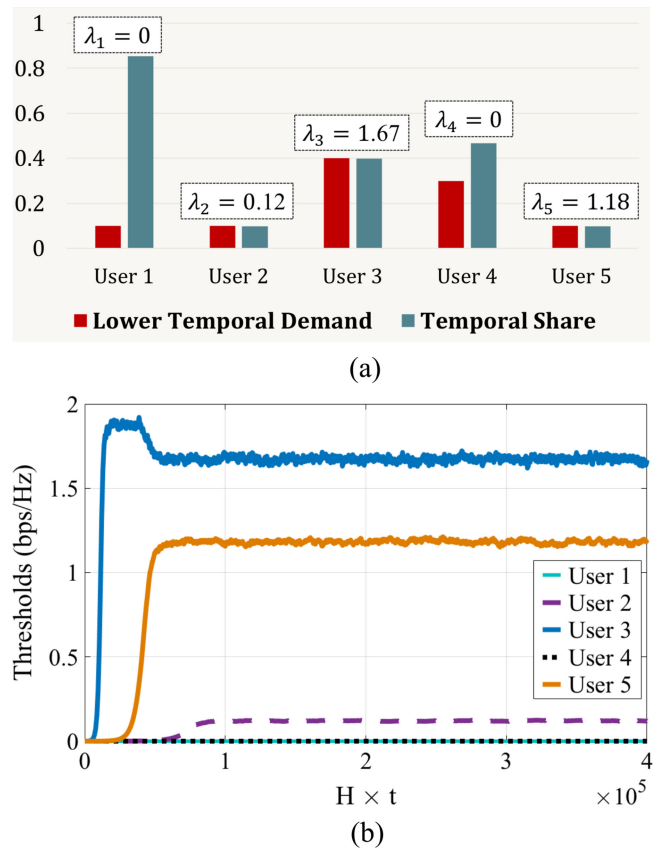


Fig. 5. (a) Long-term temporal share and the lower temporal demands of the static users. (b) The evolution of scheduling thresholds in Algorithm 2. The horizontal axis is the sampled time-slot index, where the sampling parameter H is set to 0.1.

the thresholds for users 1, 2, 4 and 5 are close to zero throughout the iterative process, whereas the threshold for user 3 increases to approximately 4 bps/Hz in a small fraction of the time-slots and fluctuates in the vicinity of 4 bps/Hz afterwards.

C. Discrete Performance Vectors

In this section, we consider a NOMA scenario with two users and discrete performance variables and discuss the effectiveness of the method described in Section VI. Due to the small number of virtual users in this scenario, we are able to find the optimal thresholds and tie-breaking decision analytically. We also use the perturbation method in Section VI to construct an ℓ -PTBS and compare the resulting performance with the optimal utility. It is shown that the utility from the method proposed in Section VI converges to the optimum utility as $\ell \rightarrow \infty$. Consider a two-user scenario where the performance values are independent discrete random variables distributed as follows:

$$R_1 = \begin{cases} 0.1 \text{ w.p. } 0.5 \\ 0.2 \text{ w.p. } 0.5 \end{cases}, \quad R_2 = \begin{cases} 0.2 \text{ w.p. } 0.5 \\ 0.3 \text{ w.p. } 0.5 \end{cases},$$

$$R_{1,2} = \begin{cases} 0.1 \text{ w.p. } 0.75 \\ 0.4 \text{ w.p. } 0.25 \end{cases}.$$

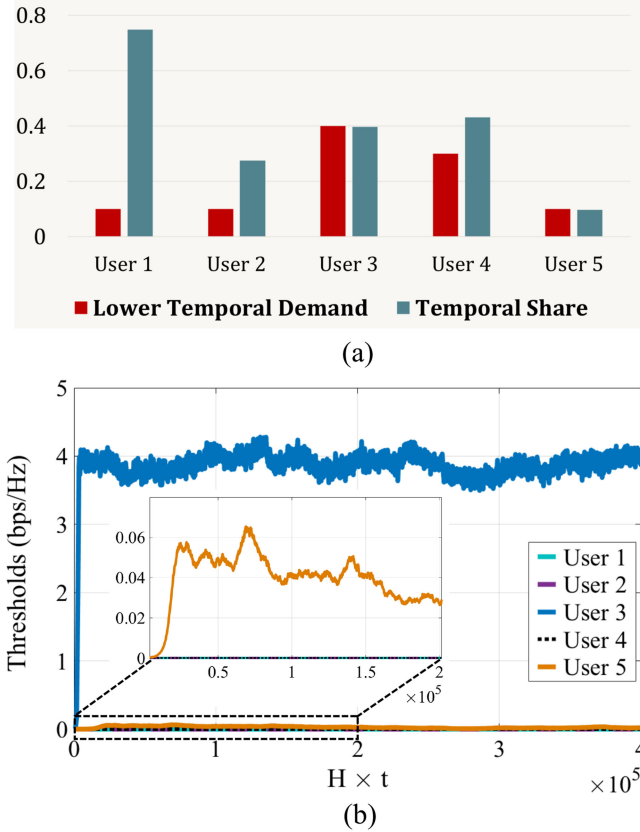


Fig. 6. (a) Long-term temporal share of the users in a mobile scenario. (b) The evolution of scheduling thresholds in time. The sampling parameter H is set to 0.1.

TABLE III
OPTIMAL TBS WITH DISCRETE PERFORMANCE VALUES

R^3	(0.1, 0.2, 0.1)	(0.1, 0.2, 0.4)	(0.1, 0.3, 0.1)	(0.1, 0.3, 0.4)
S^3	(0.2, 0.2, 0.1)	(0.2, 0.2, 0.4)	(0.2, 0.3, 0.1)	(0.2, 0.3, 0.4)
$Q(R^3)$	<i>tie</i>	$\mathcal{V}_{1,2}$	\mathcal{V}_2	$\mathcal{V}_{1,2}$
R^3	(0.2, 0.2, 0.1)	(0.2, 0.2, 0.4)	(0.2, 0.3, 0.1)	(0.2, 0.3, 0.4)
S^3	(0.3, 0.2, 0.1)	(0.3, 0.2, 0.4)	(0.3, 0.3, 0.1)	(0.3, 0.3, 0.4)
$Q(R^3)$	\mathcal{V}_1	$\mathcal{V}_{1,2}$	<i>tie</i>	$\mathcal{V}_{1,2}$

Let $w_1 = 0.5, w_2 = 0.25$. We first find the optimal thresholds and tie-breaking probability distributions analytically assuming that the channel statistics are known. For $\lambda_1 = \lambda_2 = 0$, we have $A_1^Q \leq \frac{7}{16}$. Therefore, λ_1 must be positive in order to satisfy the temporal demand of user u_1 . Take λ_1 to 0.1, Table III lists all of the possible values for the scheduling measures vector S^3 and the choice of the active user. Note that a tie happens when $R^3 = (0.1, 0.2, 0.1)$ and $R^3 = (0.2, 0.3, 0.1)$. In the former, the tie happens among all three virtual users whereas in the latter, the tie is between \mathcal{V}_1 and \mathcal{V}_2 . Let $p^3 = (p_1, p_2, p_{1,2})$ denote the tie-breaking distribution. It can be shown that an optimum tie-breaking distribution is $p^3 = (\frac{1}{3}, \frac{2}{3}, 0)$ when $R^3 = (0.1, 0.2, 0.1)$ and $p^3 = (0, 1, 0)$ when $R^3 = (0.2, 0.3, 0.1)$ by checking the sufficient conditions in Corollary 3. This gives

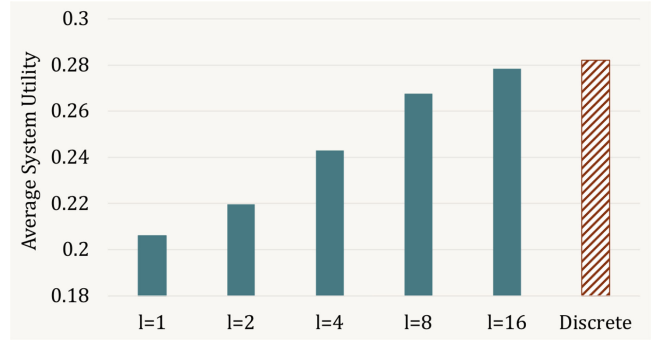


Fig. 7. Average system utility for the optimal strategy (tiled red) and the proposed method (filled green). The parameter l determines the variance of the perturbation noise which affects the discrete utility vector in the proposed method.

$A_1^Q = 0.5$ and $A_2^Q = 0.75$ which satisfy the optimality constraints described in Corollary 3. As a result, the optimal average system utility is $\frac{45}{160} \approx 0.281$. To evaluate the method proposed in Section VI, we add a vector of independent random variables with distribution $Unif[-1/l, 1/l]$ to the performance vector and use the perturbed performance values as an input to the TBS. We consider $l \in \{1, 2, 4, 8, 16\}$ and use Algorithm 2 to obtain the optimal TBS for each value of l . Figure 7 shows the average system utility for different values of l as well as for the strategy with optimal thresholds and tie-breaking distributions mentioned above. It can be seen that the average system utility converges to the optimal value as l goes to infinity.

VIII. CONCLUSION AND FUTURE WORK

In this paper, we have considered scheduling for NOMA systems under temporal demand constraints. We have shown that TBSs achieve optimal system utility and any optimal strategy is equivalent to a TBS. We have proposed a variable elimination method to find the feasible temporal share region for a given NOMA system. We have introduced an iterative algorithm based on the Robbins Monro method which finds the optimal thresholds for the TBS given the user utilities. The algorithm does not require knowledge of the users' channel statistics. Rather, it has access to the channel realizations at each time-slot. Lastly, we have provided numerical simulations to validate the proposed approach.

A natural extension to this work is multi-cell scheduling in NOMA systems. The methods proposed here may be extended and applied to centralized and distributed NOMA systems. Particularly, scheduling for multi-cell NOMA systems with limited cooperation is an interesting avenue for future work.

Another direction for future research is NOMA scheduling under short-term fairness constraints. The problem is of interest in delay sensitive applications. Short-term fairness may significantly affect the design of NOMA schedulers. It remains to be seen whether variations of TBSs can achieve near-optimal performance under short-term fairness constraints.

APPENDIX

A. Proof of Lemma 1

Let \tilde{Q} be a memoryless and stationary scheduling strategy. Since strategy \tilde{Q} is memoryless, $Q_t, t \in \mathbb{N}$ is only a function of the realization of performance vector R^m at time t . Due to stationarity, the random variables $\mathbb{1}_{\{u_i \in \tilde{Q}_t(R^{m \times t})\}}$ are independent and identically distributed (i.i.d.). From the strong law of large numbers we have:

$$\lim_{t \rightarrow \infty} A_{i,t}^{\tilde{Q}} \stackrel{a.s.}{=} \mathbb{E} \left(\mathbb{1}_{\{u_i \in \tilde{Q}_t(R^{m \times t})\}} \right) \stackrel{(a)}{=} Pr(u_i \in \tilde{Q}_t(R^m)), \quad (18)$$

where (a) follows from $\mathbb{E}(\mathbb{1}_{\mathcal{A}}) = Pr(\mathcal{A})$ for any event \mathcal{A} . Similarly, the random variables $X_t \triangleq \sum_{j=1}^m R_{j,t} \mathbb{1}_{\{\tilde{Q}_t(R^{m \times t}) = \mathcal{V}_j\}}$ are i.i.d.. Hence, from the strong law of large numbers we have:

$$\lim_{t \rightarrow \infty} U_t^{\tilde{Q}} \stackrel{a.s.}{=} \sum_{j=1}^m \mathbb{E} \left(R_j \mathbb{1}_{\{\tilde{Q}_t(R^m) = \mathcal{V}_j\}} \right). \quad (19)$$

B. Proof of Theorem 1

Case i) $w^n = \underline{w}^n = \bar{w}^n, N_{\max} = n$

As an intermediate step, we consider the special case of the scheduling problem when the temporal demand constraints must be satisfied with equality, and all subset of virtual users can be activated, i.e. $\mathbf{V} = 2^U$. It turns out that the inclusion of the joint virtual user greatly simplifies the analysis of temporally fair schedulers.

First, we prove that if a threshold strategy exists which i) satisfies the temporal constraints, and ii) for which $\lambda_i \in [-2M, 2M], \forall i \in [n]$, then it is optimal, where M is defined in Remark 1. Fix $\epsilon > 0$. Let $\epsilon' = 2nM\epsilon$. Let $\hat{Q} \in \mathcal{Q}_{TBS}$ be a TBS characterized by the threshold vector $\lambda^n \in [-2M, 2M]^n$ and let Q be an arbitrary scheduling strategy. From Equation (4) we know that $|A_i^Q - w_i| \leq \epsilon, \forall i \in [n]$. Also, by assumption, $\lambda_i \leq M, \forall i \in [n]$. As a result, $\lambda_i(A_i^Q - w_i) + \frac{\epsilon'}{n} \geq 0, \forall i \in [n]$. We have,

$$\begin{aligned} U^Q &\leq U^Q + \sum_{i=1}^n (\lambda_i(A_i^Q - w_i)) + \epsilon' \\ &\leq \liminf_{t \rightarrow \infty} \left[\frac{1}{t} \sum_{k=1}^t \sum_{j=1}^m \left(R_{j,k} \mathbb{1}_{\{Q_k(R^{m \times k}) = \mathcal{V}_j\}} \right) \right] \\ &\quad + \sum_{i=1}^n \lambda_i \cdot \liminf_{t \rightarrow \infty} \frac{1}{t} \left[\sum_{k=1}^t \left(\mathbb{1}_{\{u_i \in Q_k(R^{m \times k})\}} \right) \right] \\ &\quad - \sum_{i=1}^n \lambda_i w_i + \epsilon' \\ &\stackrel{(a)}{\leq} \liminf_{t \rightarrow \infty} \frac{1}{t} \sum_{k=1}^t \left[\sum_{j=1}^m \left(R_{j,k} \mathbb{1}_{\{Q_k(R^{m \times k}) = \mathcal{V}_j\}} \right) \right] \\ &\quad + \sum_{i=1}^n (\lambda_i \mathbb{1}_{\{u_i \in Q_k(R^{m \times k})\}}) - \sum_{i=1}^n \lambda_i w_i + \epsilon' \end{aligned}$$

$$\begin{aligned} &= \liminf_{t \rightarrow \infty} \frac{1}{t} \left[\sum_{k=1}^t \sum_{j=1}^m \left((R_{j,k} \right. \right. \\ &\quad \left. \left. + \sum_{i=1}^n \lambda_i \mathbb{1}_{\{u_i \in \mathcal{V}_j\}}) \mathbb{1}_{\{Q_k(R^{m \times k}) = \mathcal{V}_j\}} \right) \right] \\ &\quad - \sum_{i=1}^n \lambda_i w_i + \epsilon' \\ &\stackrel{(b)}{\leq} \liminf_{t \rightarrow \infty} \frac{1}{t} \left[\sum_{k=1}^t \sum_{j=1}^m \left(\left(R_{j,k} + \sum_{i=1}^n \lambda_i \mathbb{1}_{\{u_i \in \mathcal{V}_j\}} \right) \mathbb{1}_{\{\hat{Q}_k(R^{m \times k}) = \mathcal{V}_j\}} \right) \right] \\ &\quad - \sum_{i=1}^n \lambda_i w_i + \epsilon' \\ &\stackrel{(c)}{=} \liminf_{t \rightarrow \infty} \left[\frac{1}{t} \sum_{k=1}^t \sum_{j=1}^m \left(R_{j,k} \mathbb{1}_{\{\hat{Q}_k(R^{m \times k}) = \mathcal{V}_j\}} \right) \right] \\ &\quad + \sum_{i=1}^n \liminf_{t \rightarrow \infty} \frac{1}{t} \left[\sum_{k=1}^t \left(\lambda_i \mathbb{1}_{\{u_i \in \hat{Q}_k(R^{m \times k})\}} \right) \right] \\ &\quad - \sum_{i=1}^n \lambda_i w_i + \epsilon' \\ &\leq U^{\hat{Q}} + \overbrace{\sum_{i=1}^n (\lambda_i(A_i^{\hat{Q}} - w_i))}^{\leq \epsilon'} + \epsilon' = U^{\hat{Q}} + 2\epsilon', \end{aligned}$$

where (a) holds since limit inferior satisfies super-additivity, (b) holds due to the rearrangement inequality, and finally, (c) follows from the existence of the limit inferior. As a result:

$$U^Q \leq U^{\hat{Q}} + 2\epsilon', \forall \epsilon > 0, \Rightarrow U^Q \leq U^{\hat{Q}},$$

where equality holds if and only if all of the inequalities above are equalities. Particularly, equality in (b) requires that Q be equivalent with \hat{Q} .

So far, we have shown that if there exists $\hat{Q} \in \mathcal{Q}_{TBS}$ is a non-empty set, with $\lambda^n \in [-2M, 2M]^n$, then, any optimal strategy is equivalent to a threshold based strategy. In the next step, we show that at least one such \hat{Q} exists. To this end, we consider two sub-cases as follows:

Case i.1) $\sum_{i \in [n]} w_i = 1$

In this case, we show that a threshold based strategy with $\lambda_i \in [-2M, -M], \forall i \in [n]$ exists. Note that if $\lambda_i \leq -M, \forall i \in [n]$, then only the individual users (i.e. $\mathcal{V}_i = \{u_i\}, i \in [n]$) will be chosen by the threshold strategy. The reason is that the scheduling measures for the individual users are larger than that of joint users with probability one due to Remark 1. Furthermore, from [19], it is known that when individual users are chosen, one can find a set of thresholds such that $A_i^Q = w_i$ with probability one for $\sum_{i \in [n]} w_i = 1$. This shows the existence of suitable thresholds in Case i.1.

Case i.2) $\sum_{i \in [n]} w_i > 1$

To prove existence in this case, we use the following n-dimensional extension of the intermediate value theorem.

Lemma 3 (Poincaré-Miranda [34]): Let $n \in \mathbb{N}$. Consider the set of continuous functions $f_i : \mathbb{R}^n \rightarrow \mathbb{R}, i \in [n]$. Assume that for each function $f_i, i \in [n]$, there exists positive reals M_i^+ and M_i^- , such that $f_i(x^n) > 0$ if $x_i = M_i^+$ and $f_i(x^n) < 0$ if $x_i = M_i^-$. Then, the function $f^n = (f_1, f_2, \dots, f_n)$ has a root in the n-dimensional cube $\prod_{i=1}^n [-M_i^-, M_i^+]$. Alternatively:

$$\exists x_1^*, \dots, x_n^* \in \prod_{i=1}^n [-M_i^-, M_i^+] : f_i(x_1^*, \dots, x_n^*) = 0, \forall i \in [n].$$

We provide the proof when $0 < w_i < 1, i \in [n]$. Take $f_i(\lambda^n) \triangleq A_i^{Q_{TBS}} - w_i, \forall i \in [n]$. Then, f_i are continuous functions of λ^n . Next, we find a set of thresholds $(M_i^+, M_i^-), i \in [n]$ satisfying the conditions of Lemma 3. Note that if $\lambda_i = M, u_i \in Q_{TBS}(R^n)$ with probability one. To see this, let \mathcal{V}_j be a virtual user such that $u_i \notin \mathcal{V}_j$ and let $\mathcal{V}'_j = \mathcal{V}_j \cup \{u_i\}$. Then,

$$\begin{aligned} P(S(\mathcal{V}_j, R_{j,t}) \leq S(\mathcal{V}'_j, R_{j,t})) \\ = P\left(R_{j,t} + \sum_{i=1}^n \lambda_i \mathbb{1}_{\{u_i \in \mathcal{V}_j\}} \leq R'_{j,t} + \sum_{i=1}^n \lambda_i \mathbb{1}_{\{u_i \in \mathcal{V}_j\}} + M\right) \\ = P(R_{j,t} - R'_{j,t} \leq M) = 1, \end{aligned}$$

where the last equality follow from Remark 1. As a result, $A_i^{Q_{TBS}} - w_i = 1 - w_i > 0$. Hence, $M_i^+ = M$ satisfies the conditions of Lemma 3. Next, we construct $M_i^-, i \in [n]$. Note that by assumption $e \triangleq \frac{\sum_{i \in [n]} w_i - 1}{n} > 0$. Furthermore, it is straightforward to show that there exists $\alpha^n > 0$ such that $\sum_{i \in [n]} \alpha_i = 1$ and $w_i - \alpha_i e > 0, i \in [n]$. Define $w'_i = w_i - \alpha_i e, i \in [n]$. Then, by construction, $\sum_{i \in [n]} w'_i = 1$. By similar arguments as in the case i.1, for any fixed $i \in [n]$, there exists $\lambda_i \in [-2M, -M]$ such that $A_i^Q = w'_i < w_i$. So, $A_i^Q - w'_i < 0$. Consequently, $M_i^- = \lambda_i$ satisfies the condition that $f_i(\lambda^n) < 0, \lambda_i = M_i^-, \forall i \in [n]$. By Lemma 3, there exists λ^n such that $A_i^Q = w_i, i \in [n]$ simultaneously.

Case ii) $\underline{w}^n < \bar{w}^n$ or $N_{\max} < n$

The proof is broken into two subcases $\underline{w}^n = \bar{w}^n, N_{\max} < n$ and $\underline{w}^n \neq \bar{w}^n, N_{\max} \leq n$, and follows by similar arguments as Case i). The complete proof is provided in [42].

C. Proof of Theorem 3

Condition (4) follows from the properties of the Harmonic series. We provide the proof for condition (2). We showed in Theorem 1 that the optimal threshold vector λ^{*n} exists. Let ϵ^n be an arbitrary vector of real numbers. Define b_i^* and $b_i, i \in [n]$ as the resulting temporal shares for the optimal TBS with threshold vector λ^{*n} and the temporal shares for $Q_{TBS}(\lambda^n)$, respectively, where $\lambda^n = \lambda^{*n} + \epsilon^n$. Let \mathcal{A}_j^* and $\mathcal{A}_j, j \in [m]$ be the event that virtual user j is activated at a given time-slot by $Q_{TBS}(\lambda^{*n})$ and $Q_{TBS}(\lambda^n)$, respectively. We need to show that:

$$(\epsilon^n)^T (b^{*n} - b^n) > 0, \quad (20)$$

where $b_i^* = \sum_{j: u_i \in \mathcal{V}_j} P(\mathcal{A}_j^*)$, and $b_i = \sum_{j: u_i \in \mathcal{V}_j} P(\mathcal{A}_j)$. Equation (20) can be written as:

$$\sum_{i \in [n]} \epsilon_i (b_i^* - b_i) > 0. \quad (21)$$

Note that by the law of total probability

$$\begin{aligned} b_i^* &= \sum_{k \in [m]} \sum_{j: u_i \in \mathcal{V}_j} P(\mathcal{A}_j^* \cap \mathcal{A}_k), \\ b_i &= \sum_{k \in [m]} \sum_{j: u_i \in \mathcal{V}_j} P(\mathcal{A}_j \cap \mathcal{A}_k^*). \end{aligned}$$

As a result, we need to show that

$$\begin{aligned} \sum_{i \in [n]} \epsilon_i \left(\sum_{k \in [m]} \sum_{j: u_i \in \mathcal{V}_j} P(\mathcal{A}_j^* \cap \mathcal{A}_k) \right. \\ \left. - \sum_{k \in [m]} \sum_{j: u_i \in \mathcal{V}_j} P(\mathcal{A}_j \cap \mathcal{A}_k^*) \right) > 0 \\ \Leftrightarrow \sum_{k \in [m]} \sum_{i \in [n]} \sum_{j: u_i \in \mathcal{V}_j} \epsilon_i \left(P(\mathcal{A}_j^* \cap \mathcal{A}_k) - P(\mathcal{A}_j \cap \mathcal{A}_k^*) \right) > 0 \\ \Leftrightarrow \sum_{k \in [m]} \sum_{j \in [m]} \sum_{i: u_i \in \mathcal{V}_j} \epsilon_i \left(P(\mathcal{A}_j^* \cap \mathcal{A}_k) - P(\mathcal{A}_j \cap \mathcal{A}_k^*) \right) > 0 \\ \Leftrightarrow \sum_{k \in [m]} \sum_{j \in [m]} P(\mathcal{A}_j^* \cap \mathcal{A}_k) \left(\sum_{i: u_i \in \mathcal{V}_j} \epsilon_i \right) \\ - \sum_{k \in [m]} \sum_{j \in [m]} P(\mathcal{A}_j \cap \mathcal{A}_k^*) \left(\sum_{i: u_i \in \mathcal{V}_k} \epsilon_i \right) > 0. \end{aligned}$$

Let $e_j = \sum_{i: u_i \in \mathcal{V}_j} \epsilon_i, j \in [m]$. Note that e_j is the perturbation of the scheduling measure of the virtual user j defined in Definition 9 resulting from changing λ^{*n} to λ^n . In fact the scheduling measure can be written as $S(\mathcal{V}_j, R_j) = R_j + \sum_{i: u_i \in \mathcal{V}_j} \lambda_i^* + e_j$. We need to show that:

$$\begin{aligned} \sum_{k \in [m]} \sum_{j \in [m]} e_j P(\mathcal{A}_j^* \cap \mathcal{A}_k) - \sum_{k \in [m]} \sum_{j \in [m]} e_k P(\mathcal{A}_j \cap \mathcal{A}_k^*) > 0 \\ \Leftrightarrow \sum_{k \in [m]} \sum_{j \in [m]} (e_j - e_k) \left(P(\mathcal{A}_j^* \cap \mathcal{A}_k) - P(\mathcal{A}_k^* \cap \mathcal{A}_j) \right) > 0 \end{aligned}$$

We claim that $e_j - e_k$ and $P(\mathcal{A}_j^* \cap \mathcal{A}_k) - P(\mathcal{A}_k^* \cap \mathcal{A}_j)$ have the same sign for all $j, k \in [m]$. To see this, note that if $e_j > e_k$ then the threshold for virtual user j is increased more than that of virtual user k after perturbing λ^{*n} by ϵ^n . As a result, it can be shown that $P(\mathcal{A}_j^* \cap \mathcal{A}_k) > P(\mathcal{A}_k^* \cap \mathcal{A}_j)$. Roughly speaking, this can be interpreted as follows: if the threshold for virtual user j is increased more than that of virtual user k , then its temporal share increases more than that of k as well. A similar argument can be provided for $e_j < e_k$.

D. Proof of Lemma 2

Fix the pair of vectors of temporal demands $(\underline{w}^n, \bar{w}^n)$ and $(\underline{w}^m, \bar{w}^m)$ and $\alpha \in [0, 1]$. We need to show the following

inequality $U_{\underline{w}^n, \bar{w}^n}^* \geq \alpha U_{\underline{w}^n, \bar{w}^n}^* + (1 - \alpha) U_{\underline{w}^n, \bar{w}^n}^*$, where $\underline{w}^n = \alpha \underline{w}^n + (1 - \alpha) \underline{w}^n$ and $\bar{w}^n = \alpha \bar{w}^n + (1 - \alpha) \bar{w}^n$. Let Q_{TBS} be the optimal strategy for the temporal constraints $(\underline{w}^n, \bar{w}^n)$. Also, let Q'_{TBS} be the optimal strategy for the temporal constraints $(\underline{w}^n, \bar{w}^n)$. Define the strategy Q'' as follows: for α fraction of the time-slots, the strategy chooses the active user based on Q_{TBS} and for $(1 - \alpha)$ fraction of the time it uses Q'_{TBS} to choose the active user. It is straightforward to verify that the resulting temporal shares are between $(\underline{w}^n, \bar{w}^n)$. Furthermore, the resulting utility from Q'' is $U'' = \alpha U_{\underline{w}^n, \bar{w}^n}^* + (1 - \alpha) U_{\underline{w}^n, \bar{w}^n}^*$. By definition we have $U'' \leq U_{\underline{w}^n, \bar{w}^n}^*$. This completes the proof.

E. Proof of Theorem 4

We provide a sketch of the proof. Let U^* ($U_{1/\ell}^*$) be the optimal strategy for the setup Ω_0 ($\Omega_{1/\ell}$) achieved using the strategy Q^* ($Q_{1/\ell}^*$). Furthermore, let $U_{1/\ell}$ be the utility due to applying the ℓ -PTBS $\hat{Q}_{1/\ell}$ to Ω_0 . We need to show that the sequence $U_{1/\ell}$ converges to U^* in probability as $\ell \rightarrow \infty$. The sequence $U_{1/\ell}$ is upper-bounded by U^* by definition of U^* . Consequently, to prove Theorem 4, it is enough to show that $P(U^* \leq U_{1/\ell} + \frac{2}{\ell}) = 1$. In order to prove the last equality we consider an intermediate *genie-assisted* strategy $\tilde{Q}_{1/\ell}$ for the setup $\Omega_{1/\ell}$. The strategy uses the output of Q^* as side-information assuming that the output is provided using a genie. More precisely, at time-slot t the strategy $\tilde{Q}_{1/\ell}$ for $\Omega_{1/\ell}$ activates the same virtual user \mathcal{V}_j which the strategy Q^* activates for Ω_0 . Let $\tilde{U}_{1/\ell}$ be the average utility of $\tilde{Q}_{1/\ell}$. Then, $U^* \leq \tilde{U}_{1/\ell} + \frac{1}{\ell}$ with probability one. The reason is that the two strategies activate the same virtual users and the utility in Ω_0 and $\Omega_{1/\ell}$ differ in a $Unif[-1/\ell, 1/\ell]$ variable for any given virtual user. On the other hand, using the rearrangement inequality as in the proof of Theorem 1, it can be shown that $P(\tilde{U}_{1/\ell} \leq U_{1/\ell}^*) = 1$. Furthermore, $U_{1/\ell}^* \leq U_{1/\ell} + \frac{1}{\ell}$ by similar arguments. As a result,

$$\begin{aligned} P\left(U^* \leq U_{1/\ell} + \frac{2}{\ell}\right) &\geq P\left(U^* \leq U_{1/\ell}^* + \frac{1}{\ell}\right) \\ &\geq P\left(U^* \leq \tilde{U}_{1/\ell} + \frac{1}{\ell}\right) = 1 \Rightarrow P\left(U^* \leq U_{1/\ell} + \frac{2}{\ell}\right) = 1. \end{aligned}$$

The proof is completed by taking ℓ to infinity.

ACKNOWLEDGMENT

The authors would like to thank Dr. Mohammad A. Khojastepour from NEC Laboratories America for his constructive comments.

REFERENCES

- [1] L. Dai, B. Wang, Z. Ding, Z. Wang, S. Chen, and L. Hanzo, "A survey of non-orthogonal multiple access for 5G," *IEEE Commun. Surv. Tut.*, vol. 20, no. 3, pp. 2294–2323, Thirdquarter 2018.
- [2] Y. Saito, A. Benjebbour, Y. Kishiyama, and T. Nakamura, "System-level performance evaluation of downlink non-orthogonal multiple access (NOMA)," in *Proc. IEEE 24th Int. Symp. Pers. Indoor Mobile Radio Commun.*, 2013, pp. 611–615.
- [3] Z. Ding *et al.*, "Application of non-orthogonal multiple access in LTE and 5G networks," *IEEE Commun. Mag.*, vol. 55, no. 2, pp. 185–191, Feb. 2017.
- [4] Z. Ding, X. Lei, G. K. Karagiannidis, R. Schober, J. Yuan, and V. Bhargava, "A survey on non-orthogonal multiple access for 5G networks: Research challenges and future trends," 2017, arXiv:1706.05347.
- [5] K. Seong, M. Mohseni, and J. M. Cioffi, "Optimal resource allocation for OFDMA downlink systems," in *Proc. IEEE Int. Symp. Inf. Theory*, 2006, pp. 1394–1398.
- [6] Z. Ding, R. Schober, and H. V. Poor, "A general MIMO framework for NOMA downlink and uplink transmission based on signal alignment," *IEEE Trans. Wireless Commun.*, vol. 15, no. 6, pp. 4438–4454, Jun. 2016.
- [7] N. Otao, Y. Kishiyama, and K. Higuchi, "Performance of non-orthogonal access with SIC in cellular downlink using proportional fair-based resource allocation," in *Proc. Int. Symp. Wireless Commun. Syst.*, 2012, pp. 476–480.
- [8] S. M. R. Islam, M. Zeng, O. A. Dobre, and K. S. Kwak, "Resource allocation for downlink NOMA systems: Key techniques and open issues," *IEEE Wireless Commun.*, vol. 25, no. 2, pp. 40–47, Apr. 2018.
- [9] W. Yu and J. M. Cioffi, "Sum capacity of Gaussian vector broadcast channels," *IEEE Trans. Inf. Theory*, vol. 50, no. 9, pp. 1875–1892, Sep. 2004.
- [10] L. Lei, D. Yuan, C. K. Ho, and S. Sun, "Power and channel allocation for non-orthogonal multiple access in 5G systems: Tractability and computation," *IEEE Trans. Wireless Commun.*, vol. 15, no. 12, pp. 8580–8594, Dec. 2016.
- [11] Y. Liu, M. ElKashlan, Z. Ding, and G. K. Karagiannidis, "Fairness of user clustering in MIMO non-orthogonal multiple access systems," *IEEE Commun. Lett.*, vol. 20, no. 7, pp. 1465–1468, Jul. 2016.
- [12] Z. Yang, Z. Ding, P. Fan, and N. Al-Dhahir, "A general power allocation scheme to guarantee quality of service in downlink and uplink NOMA systems," *IEEE Trans. Wireless Commun.*, vol. 15, no. 11, pp. 7244–7257, Nov. 2016.
- [13] J. Cui, Y. Liu, Z. Ding, P. Fan, and A. Nallanathan, "Optimal user scheduling and power allocation for millimeter wave NOMA systems," *IEEE Trans. Wireless Commun.*, vol. 17, no. 3, pp. 1502–1517, Mar. 2018.
- [14] Y. Saito, Y. Kishiyama, A. Benjebbour, T. Nakamura, A. Li, and K. Higuchi, "Non-orthogonal multiple access (NOMA) for cellular future radio access," in *Proc. IEEE 77th Veh. Technol. Conf.*, 2013, pp. 1–5.
- [15] X. Liu, E. K. Chong, and N. B. Shroff, "A framework for opportunistic scheduling in wireless networks," *Elsevier Comput. Netw.*, vol. 41, no. 4, pp. 451–474, 2003.
- [16] Z. Zhang, Y. He, and E. K. Chong, "Opportunistic scheduling for OFDM systems with fairness constraints," *EURASIP J. Wireless Commun. Netw.*, vol. 2008, 2008, Art. no. 25.
- [17] F. P. Kelly, A. K. Maulloo, and D. K. Tan, "Rate control for communication networks: Shadow prices, proportional fairness and stability," *J. Oper. Res. Soc.*, vol. 49, no. 3, pp. 237–252, 1998.
- [18] P. Viswanath, D. N. C. Tse, and R. Laroia, "Opportunistic beamforming using dumb antennas," *IEEE Trans. Inf. Theory*, vol. 48, no. 6, pp. 1277–1294, Jun. 2002.
- [19] X. Liu, E. K. P. Chong, and N. B. Shroff, "Opportunistic transmission scheduling with resource-sharing constraints in wireless networks," *IEEE J. Sel. Areas Commun.*, vol. 19, no. 10, pp. 2053–2064, Oct. 2001.
- [20] S. S. Kulkarni and C. Rosenberg, "Opportunistic scheduling for wireless systems with multiple interfaces and multiple constraints," in *Proc. ACM Int. Workshop Model. Anal. Simul. Wireless Mobile Syst.*, 2003, pp. 11–19.
- [21] T. Issariyakul and E. Hossain, "Throughput and temporal fairness optimization in a multi-rate TDMA wireless network," in *Proc. IEEE Int. Conf. Commun.*, vol. 7, 2004, pp. 4118–4122.
- [22] A. Asadi and V. Mancuso, "A survey on opportunistic scheduling in wireless communications," *IEEE Commun. Surv. Tut.*, vol. 15, no. 4, pp. 1671–1688, Fourth Quarter 2013.
- [23] G. Tan and J. V. Gutttag, "Time-based fairness improves performance in multi-rate WLANs," in *Proc. USENIX Annu. Tech. Conf., General Track*, 2004, pp. 269–282.
- [24] T. Joshi, A. Mukherjee, Y. Yoo, and D. P. Agrawal, "Airtime fairness for IEEE 802.11 multirate networks," *IEEE Trans. Mobile Comput.*, vol. 7, no. 4, pp. 513–527, Apr. 2008.
- [25] S. Shahsavari and N. Akar, "A two-level temporal fair scheduler for multicell wireless networks," *IEEE Wireless Commun. Lett.*, vol. 4, no. 3, pp. 269–272, Jun. 2015.
- [26] S. Shahsavari, N. Akar, and B. H. Khalaj, "Joint cell muting and user scheduling in multicell networks with temporal fairness," *Wireless Commun. Mobile Comput.*, vol. 2018, 2018, Art. no. 4846291.

- [27] Z. Wei, D. W. K. Ng, and J. Yuan, "Power-efficient resource allocation for MC-NOMA with statistical channel state information," in *Proc. IEEE Global Commun. Conf.*, 2016, pp. 1–7.
- [28] W. Liang, Z. Ding, Y. Li, and L. Song, "User pairing for downlink non-orthogonal multiple access networks using matching algorithm," *IEEE Trans. Commun.*, vol. 65, no. 12, pp. 5319–5332, Dec. 2017.
- [29] X. Chen, A. Benjebbour, A. Li, and A. Harada, "Multi-user proportional fair scheduling for uplink non-orthogonal multiple access (NOMA)," in *Proc. 79th IEEE Veh. Technol. Conf.*, 2014, pp. 1–5.
- [30] T. S. Rappaport, *et al.*, *Wireless Commun.: Principles and Practice*, vol. 2. NJ, USA: Prentice Hall, 1996.
- [31] S. R. Islam, N. Avazov, O. A. Dobre, and K.-S. Kwak, "Power-domain non-orthogonal multiple access (NOMA) in 5G systems: Potentials and challenges," *IEEE Commun. Surv. Tut.*, vol. 19, no. 2, pp. 721–742, Secondquarter 2017.
- [32] P. Bergmans, "A simple converse for broadcast channels with additive white Gaussian noise (corresp.)," *IEEE Trans. Inf. Theory*, vol. IT-20, no. 2, pp. 279–280, Mar. 1974.
- [33] B. Hassibi and M. Sharif, "Fundamental limits in MIMO broadcast channels," *IEEE J. Sel. Areas Commun.*, vol. 25, no. 7, pp. 1333–1344, Sep. 2007.
- [34] W. Kulpa, "The Poincaré-Miranda theorem," *Amer. Math. Monthly*, vol. 104, pp. 545–550, 1997.
- [35] X. Allamigeon, U. Fahrenberg, S. Gaubert, R. D. Katz, and A. Legay, "Tropical Fourier-Motzkin elimination, with an application to real-time verification," *Int. J. Algebra Comput.*, vol. 24, no. 05, pp. 569–607, 2014.
- [36] F. S. Chaharsooghi, M. J. Emadi, M. Zamanighomi, and M. R. Aref, "A new method for variable elimination in systems of inequations," in *Proc. IEEE Int. Symp. Inf. Theory*, 2011, pp. 1215–1219.
- [37] R. Koch, "Affine monoids, Hilbert bases and Hilbert functions," Department of Mathematics / Computer Science, Ph.D. dissertation, Osnabrück University, Osnabrück, Germany, 2003.
- [38] H. Robbins and S. Monro, "A stochastic approximation method," *Ann. Math. Statist.*, vol. 22, pp. 400–407, 1951.
- [39] D. Ruppert, "A Newton-Raphson version of the multivariate robbins-monro procedure," *Ann. Statist.*, vol. 13, pp. 236–245, 1985.
- [40] D. P. Bertsekas, *Nonlinear Programming*. Belmont, MA, USA: Athena scientific, 2016.
- [41] 3GPP, "LTE; Evolved Universal Terrestrial Radio Access (E-UTRA); Physical layer procedures (TS 36.213 version 12.4.0 release 12)," European Telecommunications Standards Institute, Sophia Antipolis, France, Rep. No. RTS/TSGR-0136213vc40, 2015.
- [42] S. Shahsavari, F. Shirani, and E. Erkip, "A general framework for temporal fair user scheduling in NOMA systems," 2018, arXiv:1809.06431.



Shahram Shahsavari received the B.S. degree in electrical engineering from the Amirkabir University of Technology (Tehran Polytechnic), Iran, in 2013, and the M.S. degree in electrical engineering from the Sharif University of Technology, Iran, in 2015. He received the Ph.D. degree in electrical engineering from the New York University Tandon School of Engineering, NY, USA, in 2019. He is also with NYU WIRELESS Center at New York University conducting research on next generation wireless networks.

His research interests include wireless communications, modern cellular systems, radio resource management, and network optimization. Dr. Shahsavari was the recipient of NYU Ernst Weber fellowship in 2015.



Farhad Shirani received the B.Sc. degree in electrical engineering from the Sharif University of Technology, Tehran, Iran, in 2011, and the M.Sc. and Ph.D. degrees from the University of Michigan, Ann Arbor, MI, USA, in 2016. He also received the M.Sc. degree in mathematics from the University of Michigan in 2016. He served as a Lecturer and Postdoctoral Research Fellow with the University of Michigan in 2017. Currently, he is a Research Assistant Professor with the New York University at New York, NY, USA. His recent works include developing information theoretic methods for analysis of fundamental limits of web privacy, design of receiver architectures for energy efficient communication over MIMO systems, and design of algorithms for opportunistic multi-user scheduling under various fairness constraints. His research interests include privacy and security, wireless communications, and multi-terminal communication systems.



Elza Erkip received the B.S. degree in electrical and electronics engineering from Middle East Technical University, Ankara, Turkey, and the M.S. and the Ph.D. degrees in electrical engineering from Stanford University, Stanford, CA, USA. She is an Institute Professor with the Electrical and Computer Engineering Department at the New York University Tandon School of Engineering, NY, USA. Her research interests are in information theory, communication theory, and wireless communications.

Dr. Erkip is a member of the Science Academy of Turkey and is a Clarivate Highly Cited Researcher. She was the recipient of the NSF CAREER Award in 2001, the IEEE Communications Society WICE Outstanding Achievement Award in 2016, and the IEEE Communications Society Communication Theory Technical Committee (CTTC) Technical Achievement Award in 2018. Her paper awards include the IEEE Communications Society Stephen O. Rice Paper Prize in 2004, and the IEEE Communications Society Award for Advances in Communication in 2013. She has been a member of the Board of Governors of the IEEE Information Theory Society since 2012 where in 2018, she was the Society President. She was a Distinguished Lecturer of the IEEE Information Theory Society from 2013 to 2014.

She has had many editorial and conference organization responsibilities. Some recent ones include Asilomar Conference on Signals, Systems and Computers, MIMO Communications and Signal Processing Track Chair in 2017, IEEE Wireless Communications and Networking Conference Technical Co-Chair in 2017, IEEE JOURNAL ON SELECTED AREAS IN COMMUNICATIONS Guest Editor in 2015, and IEEE International Symposium of Information Theory General Co-Chair in 2013.